ADVANCES IN MATERIALS DEVELOPMENT OF RESPONSIVE PHOTONIC CRYSTAL HYDROGELS

by

Michelle Marie Ward Muscatello

B.S., University of North Dakota, 1994

M.S., University of Pittsburgh, 2003

Submitted to the Graduate Faculty of

Arts and Sciences in partial fulfillment

of the requirements for the degree of

Doctor of Philosophy

University of Pittsburgh

2009

UNIVERSITY OF PITTSBURGH

ARTS AND SCIENCES

This dissertation was presented

by

Michelle M. Ward Muscatello

It was defended on

December 18, 2008

and approved by

Adrian C. Michael, Associate Professor, Department of Chemistry

Stephen G. Weber, Professor, Department of Chemistry

David N. Finegold, Professor, Department of Pediatrics

Dissertation Advisor: Sanford A. Asher, Distinguished Professor, Department of Chemistry

ADVANCES IN MATERIALS DEVELOPMENT OF RESPONSIVE PHOTONIC

CRYSTAL HYDROGELS

Michelle M. Ward Muscatello, PhD

University of Pittsburgh, 2009

We advanced the material development of our responsive photonic crystal hydrogels, which are utilized in our polymerized crystalline colloidal array (PCCA) technology. PCCA consist of a hydrogel network that embeds an array of monodisperse, highly-charged 100-200 nm polystyrene particles. The optical properties of the embedded array are such that it Bragg diffracts visible light. Responsive materials are fabricated by exploiting the volume-responsive nature of the hydrogel network, such that the material is functionalized to respond to a specific analyte of interest by actuating a volume change in the hydrogel, resulting in a change in the color of diffracted light.

We prepared a new hydrogel system for the preparation of responsive PCCA based on the biocompatible and rehydratable polymer polyvinyl alcohol (PVA). This material can be reversibly dehydrated and rehydrated, without the use of fillers, while retaining the diffraction and swelling properties of polymerized crystalline colloidal arrays. This reversibility of rehydration of this new hydrogel material enables practical storage of hydrogel-based photonic crystal sensors in the dry state, which makes them much more useful for future commercial applications.

We continued the development of our PCCA glucose sensing materials for application in monitoring relatively high glucose concentrations, such as found in blood. We modified our synthetic fabrication methodologies in order to increase the reproducibility of our sensing

materials. We advanced our understanding of the sensing response by utilizing independently determined variables in our modeling of the PCCA diffraction response. We characterized our material's response dependence upon environmental variations and interferences.

We completed the first quantitative study of how the mechanical properties of a swollen hydrogel depend upon the size of nonbonded embedded nanoparticles. We experimentally determined the dependence of the elastic shear storage modulus for our PCCA, as a function of embedded CCA size and prepolymerization conditions, and found that the modulus increases linearly with increasing CCA size due to interaction between the embedded nanoparticles and the hydrogel matrix. The effective hydrogel crosslink densities determined from these storage modulus values indicate that we can affect the responsivity of our photonic crystal materials by controlling the included nanoparticle size.

TABLE OF CONTENTS

LIST OF TABLES

LIST OF FIGURES

constants of the bound complexes are affected by the attached hydrogel and that solution equilibria are too simplistic to successfully model the interactions within the hydrogel matrix.. 54

PREFACE

I would like thank my research advisor, Professor Sanford Asher, for his advice and guidance throughout my graduate studies. He saw something in a naive school teacher many years ago and provided me with the opportunity to grow into the scientist I am today. I cannot express my deep gratitude for all that he has done for me. My world is so much bigger and richer than it was when I first walked into his office.

I would like to thank the members of the Asher Research Group, both past and present, for their collaborations and friendship. That which I have learned by working with such a clever, capable, and kind group abounds over anything that I had ever been taught inside a classroom. There have been too many good people I have worked with over the years to list them all individually; however, there are a special few I must single out. I would like to specifically mention Vladimir Alexeev who was a truly generous mentor, inspiration and friend. His untimely death is a loss I will always feel. Special thanks to Lee Stunja, whose collaboration and friendship made my final years here much more enjoyable. I would also like to thank Sharon Mansfield for her constant friendship and encouragement – everyone should be so fortunate to have a Sharon in their lives.

I consider myself very fortunate to have had the opportunity to study in this chemistry department. Our faculty is not only brilliant, but they are also truly approachable and genuinely invest of themselves in their students. I am proud and humbled to possess a degree gained in the presence of such scholars. I would like to specifically thank the members of my comprehensive,

As I look back over my time here at the University of Pittsburgh, I can't help but be thankful for the "broken roads" that have led me to this point in my life. I am blessed indeed.

1.0   INTRODUCTION

1.1   BACKGROUND

Hydrogels are crosslinked polymers, which are capable of absorbing large volumes of water in a three dimensional network of polymer chains. The network properties of these materials are influenced by the nature of the polymer constituents and crosslinks[1,2]. Because of their unique properties, and the ability to tune these properties, polymeric hydrogels have found widespread applications in the biomedical field[3-5], including tissue engineering[6-8], drug delivery[9-11], protein separation[12-15], contact lenses[16,17], and biomedical devices[18-20].

For the past several decades, researchers have worked on the development of stimuli-sensitive hydrogels or "smart" hydrogels[15,18,20-47]. Smart hydrogels are materials that are capable of undergoing a relatively large reversible property change in response to a small environmental change. Polymeric hydrogels have been designed to respond to diverse physical and chemical stimuli, including pH[28,29,38], temperature[15,30,31], light[32,33,37], and magnetic field[34-36].

The Asher Research Group at the University of Pittsburgh has significantly contributed to the development of responsive hydrogels through the development of polymerized crystalline colloidal arrays (PCCA)[40,43,44,48-51]. PCCA are photonic crystal materials composed of a hydrogel network which embeds a crystalline colloidal array (CCA)[52-59]. These materials take advantage of the optical properties of the embedded CCA, such that their response to a specific

1

analyte of interest actuates a change in the color of light diffracted by the material. Current research in the area of intelligent PCCA (IPCCA) materials has focused on chemical sensing applications, which exploit the volume-responsive nature of the hydrogel network, leading to the development of sensors for the detection of multiple analytes, including glucose[47,60-63], cations[42,45,46,64], ammonia[65], pH[38,66], organophosphates[39,67], and creatinine[41].

1.2   CCA: PREPARATION, SELF-ASSEMBLY, AND BRAGG DIFFRACTION

The polystyrene particles which comprise the crystalline colloidal arrays are typically synthesized through a free-radical emulsion polymerization[54]. This synthesis can be used to prepare particles that are between 100–400 nm in diameter (Figure 1-1A). The reactants for the polymerization include an emulsifier, slightly water-soluble monomers, a less water-soluble crosslinker, a water-soluble initiator, and a buffer in an aqueous polymerization medium. The surface charge and size of the resulting particles can be altered by varying the relative amounts of these reactants.

Aqueous suspensions of these monodisperse, highly-charged particles self-assemble into highly-ordered three-dimensional arrays in low ionic strength media due to electrostatic repulsion, originating from the ionization of acid groups on the surface of each particle (Figure 1-1B). The system minimizes its free energy by assembling into either a face-centered cubic (FCC) or body-centered cubic (BCC) lattice, based upon the particle size and concentration (Figure 1-1C)[58,59]. The periodic modulation in the CCA refractive index and the lattice spacing of the array are such that visible light is diffracted according to Bragg's Law:

$$m\lambda_0 = 2nd \sin\theta$$

Equation 1-1

where m is the order of diffraction, λ_0 is the diffracted wavelength, n is the refractive index of the system, d is the spacing between the diffracting planes and θ is the glancing angle between the direction of propagation of the incident light and the diffracting planes (Figure 1-2)[58,59]. The lattice spacing of the CCA can be tuned, either by changing the particle size or the particle concentration, so that CCA can efficiently diffract light in the near-UV, visible and near-IR spectral regions.
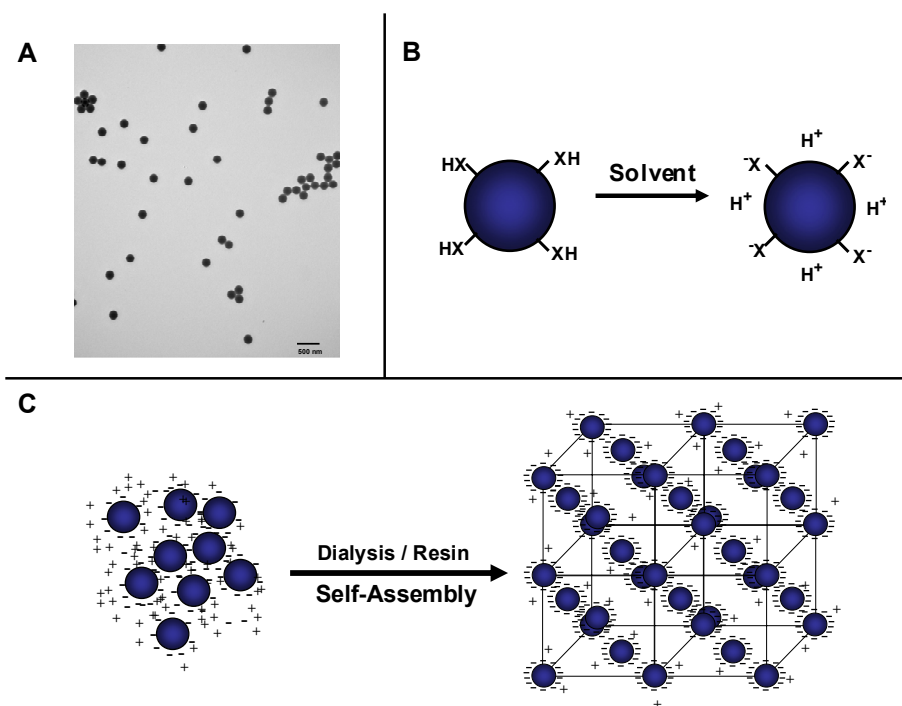
Figure 1-1. (A) Transmission electron micrograph of highly monodisperse, highly charged 186 nm polystyrene colloidal particles. (Scale bar indicates 500 nm.) (B) In an aqueous solvent, the acid groups present on the particle surface dissociate. (C) After removing ionic contaminants from the solution, via dialysis and ion exchange resin, the particles self-assemble into a 3-dimentional crystal lattice, termed crystalline colloidal array (CCA).

A

diffracted light
λ_0

normal to (111)

incident light

θ_B

$$m\lambda_0 = 2nd \sin \theta_B$$

m: order of diffraction

λ_0: wavelength of diffracted light

n: refractive index of system

d: spacing between diffracting planes

θ_B: Bragg glancing angle

B

Diffracted Intensity, I_D

500 550 600 650 700 750 800 850
Wavelength / nm

$$\lambda = 2nd$$
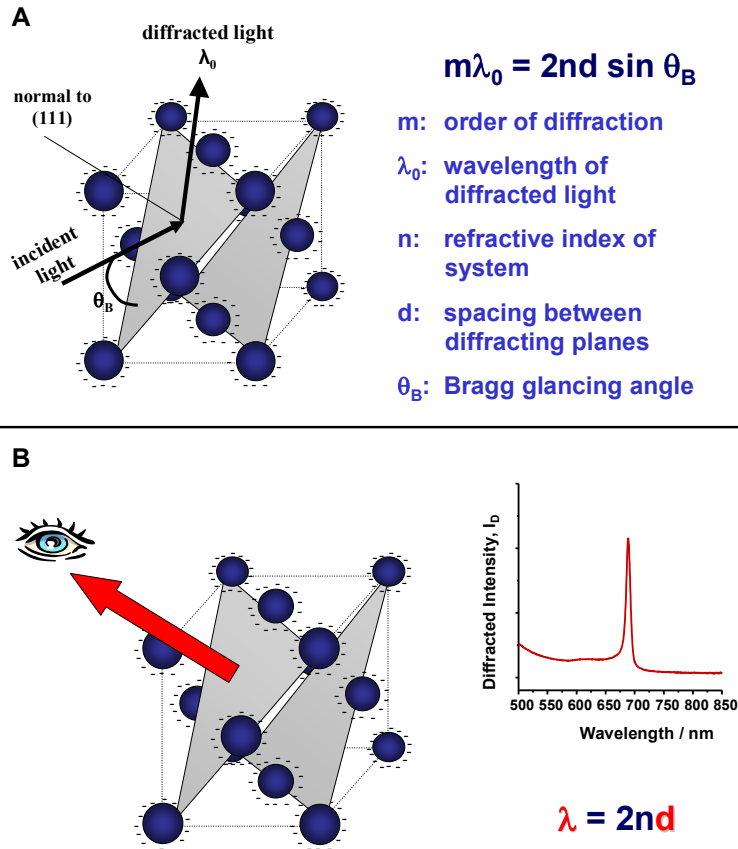
Figure 1-2. (A) The periodic modulation in the CCA refractive index and the lattice spacing of the array are such that visible light is diffracted according to Bragg's Law. (B) By fixing the Bragg glancing angle to 90°, the observed diffraction from the lattice is derived primarily from the spacing between the diffracting planes.

1.3   PCCA FABRICATION AND RESPONSE ELUCIDATION

Since the ordering of the CCA depends on the electrostatic repulsion between particles, the lattice will disorder in the presence of ionic impurities. As many analytes of interest are ionic in nature themselves or occur in ionic solutions, such as bodily fluids, this instability of the CCA

4

lattice must be overcome in order to take advantage of the distinctive optical properties for sensor material development. The CCA lattice is stabilized by polymerizing it within a hydrogel to form a polymerized crystalline colloidal array (PCCA) (Figure 1-3)[51,55].
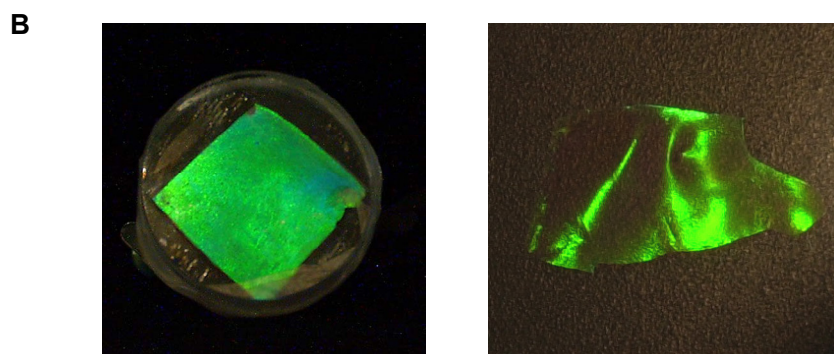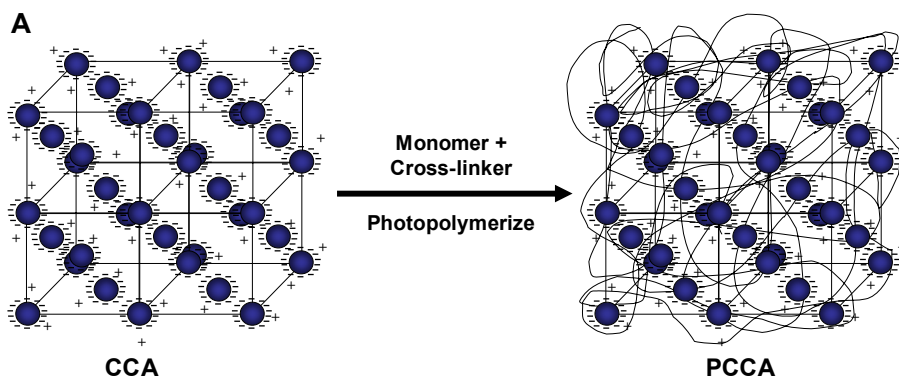
Figure 1-3. (A) During a UV-initiated free radical polymerization, the crystalline colloidal array (CCA) is embedded within a hydrogel matrix forming a polyermized crystalline colloidal array (PCCA). (B) On the left is a picture of a prepolymerization solution of monomer, crosslinker, initiator, and CCA within two quartz plates. On the right is a picture of the polymerized hydrogel floating in water. The diffraction exhibited in the prepolymerization solution is maintained in the resulting hydrogel.

The PCCA is prepared via a UV-initiated free radical polymerization of a nonionic monomer and crosslinker, such as acrylamide and bisacrylamide, which are dissolved into the

CCA. The resulting PCCA is considerably more robust than the CCA. Additionally, as the CCA lattice is embedded within the hydrogel, the observed diffraction closely follows the hydrogel volume. As the hydrogel undergoes a volume change, the spacing between the embedded diffracting lattice planes will change, resulting in a change in the observed wavelength of diffraction[44,48-50].
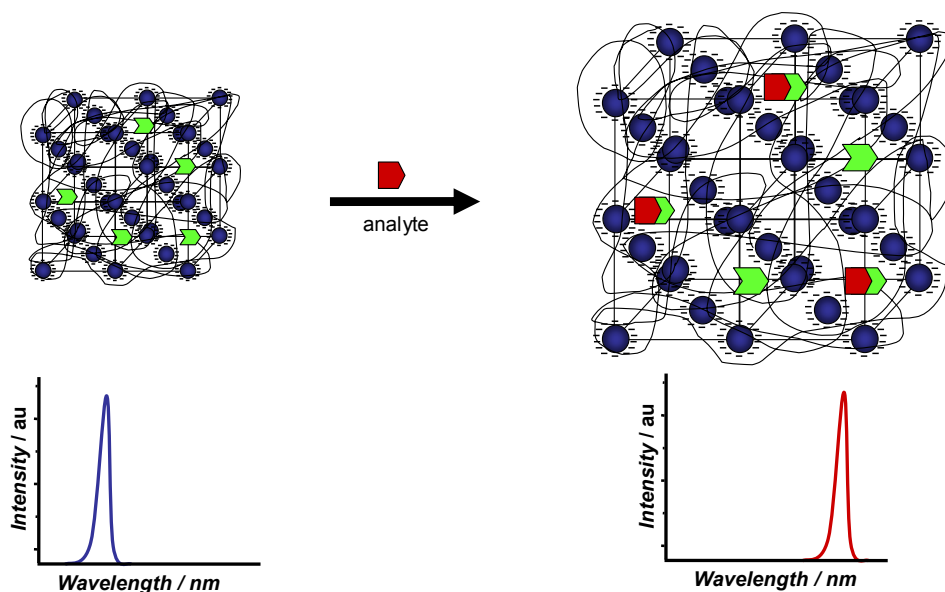
Figure 1-4. Intelligent PCCA (IPCCA) optically report on the concentration of the analyte of interest through diffraction changes that result from hydrogel swelling (shown above) or shrinking. As the analyte of interest is bound, there will be a change in the free energy of the system, resulting in a change in the equilibrium volume of the hydrogel. As the hydrogel swells, the spacing between the diffracting planes of the embedded CCA increases, red-shifting the wavelength of light diffracted by the material proportionate to the amount of analyte bound.

The volume-responsive nature of the polymeric hydrogel is exploited for chemical sensing applications by incorporating molecular recognition groups onto the polymer backbone either during or after polymerization. The resulting intelligent PCCA (IPCCA) optically reports on the concentration of the analyte of interest through diffraction changes that result from

6

hydrogel swelling or shrinking (Figure 1-4)[44,48-50]. As the analyte of interest is bound, there will

be a change in the free energy of the system, resulting in a change in the equilibrium volume of

the hydrogel.

$$\Pi_M = -\frac{\partial \Delta G_M}{\partial V} = -\frac{RT}{V_s}\left[\ln\left(1-\frac{V_0}{V}\right)+\frac{V_0}{V}+\chi\left(\frac{V_0}{V}\right)^2\right]$$

$$\Pi_T = \Pi_M + \Pi_E + \Pi_{Ion} = 0$$

$$\Pi_{Ion} = RT(c_+ + c_- - c_+^* - c_-^*)$$

$$\Pi_E = -\frac{\partial \Delta G_E}{\partial V} = -RT\cdot\upsilon_e\left[\left(\frac{V_m}{V}\right)^{1/3}-\frac{1}{2}\frac{V_m}{V}\right]-RT\cdot c_{add}$$

Figure 1-5. The volume changes experienced by the photonic crystal hydrogel material can be
understood by utilizing Flory's model for the swelling of polymer network structures. At
equilibrium, the total osmotic pressure of the network equals zero. (R is the universal gas
constant, T is the temperature, χ is the Flory-Huggins interaction parameter, V_s is the molar
volume of the solvent, υ_e is the effective crosslink density of the hydrogel network, c_{add} is the
concentration of additional crosslinks formed upon analyte binding, V is the current volume of the
hydrogel, V_m is the volume of the relaxed hydrogel network, V_0 is the volume of the dry hydrogel
network, c_+ and c_- are the concentrations of mobile cations and anions inside the hydrogel, and c_+^*
and c_-^* are the concentrations of mobile cations and anions outside the hydrogel.)

The volume change experienced by these hydrogels can be explained by considering the

individual contributions to the change in the total free energy of the system (ΔG_{tot}):

$$\Delta G_{tot} = \Delta G_{mix} + \Delta G_{elas} + \Delta G_{ion}$$

Equation 1-2

and the resulting osmostic pressure (Π_{tot}):

$$\Pi_{tot} = \Pi_{mix} + \Pi_{elas} + \Pi_{ion}$$

Equation 1-3

where ΔG_{mix} is the change in the free energy of mixing, ΔG_{elas} is the change in the elastic free energy, and ΔG_{ion} is the change in free energy associated with ionic interactions (Figure 1-5)[1,2]. IPCCA can be designed to respond to changes in each of the free energy terms.

A

$$\Pi_{\mathrm{M}} = -\frac{\partial \Delta G_{\mathrm{M}}}{\partial V} = -\frac{RT}{V_s}\left[\ln\left(1-\frac{V_0}{V}\right) + \frac{V_0}{V} + \chi\left(\frac{V_0}{V}\right)^2\right]$$

B
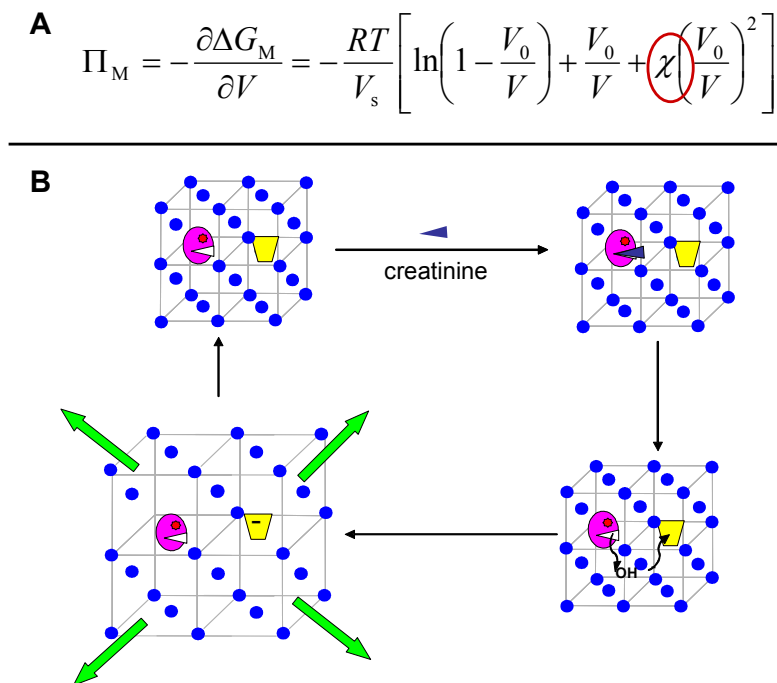
creatinine

Figure 1-6. (A) The osmotic pressure resulting from changes in the free energy of mixing derives from changes in the Flory-Huggins interaction parameter (χ), which is a measure of the interaction of a polymer with a solvent. (B) The creatinine sensor utilizes an enzyme that hydrolyzes creatinine and a titratable phenol group tethered to the hydrogel backbone. As the creatinine is hydrolyzed, the phenol groups are titrated to more soluble phenolate groups, resulting in a swelling of the hydrogel and red-shifting of the diffraction in proportion to the concentration of creatinine hydrolyzed.

The osmotic pressure resulting from changes in the free energy of mixing derives from changes in the Flory-Huggins interaction parameter (χ), which is a measure of the interaction of a polymer with a solvent (Figure 1-6A)[1,2]. This can be thought of as the solubility of the polymer matrix within the surrounding solvent, such that alterations to the solubility of the polymer will result in hydrogel volume changes, thereby shifting the wavelength of diffraction. An IPCCA that responds to changes in the free energy of mixing is illustrated by the creatinine sensor (Figure 1-6B)[41]. This material utilizes an enzyme that hydrolyzes creatinine and a titratable phenol group tethered to the hydrogel backbone. As the creatinine is hydrolyzed, the phenol groups are titrated to more soluble phenolate groups, resulting in a swelling of the hydrogel and red-shifting of the diffraction in proportion to the concentration of creatinine hydrolyzed.

Changes in the free energy of elasticity derive from changes in the concentration of effective crosslinks within the hydrogel network (Figure 1-7A)[1,2]. Within the hydrogel, there are two forms of crosslinks: permanent (crosslinks formed during the photopolymerization of the polymer network) and temporary (crosslinks formed during the binding of the analyte of interest). Incorporation of a ligand capable of forming "sandwich" complexes with the analyte of interest will result in an increase of effective crosslinks within the hydrogel network, shrinking the hydrogel, and blue-shifting the wavelength of diffraction. An IPCCA that responds to changes in the free energy of elasticity is the glucose sensor, which utilizes boronic acid recognition molecules tethered to the PCCA hydrogel backbone (Figure 1-7B)[47]. Upon binding glucose, additional bisboronate-glucose crosslinks are formed within this originally lightly crosslinked hydrogel, shrinking the hydrogel volume in proportion to the concentration of glucose.

A

$$\Pi_E = -\frac{\partial \Delta G_E}{\partial V} = -RT \cdot \upsilon_e \left[\left(\frac{V_m}{V} \right)^{1/3} - \frac{1}{2} \frac{V_m}{V} \right] - RT \cdot c_{B2G}$$

B
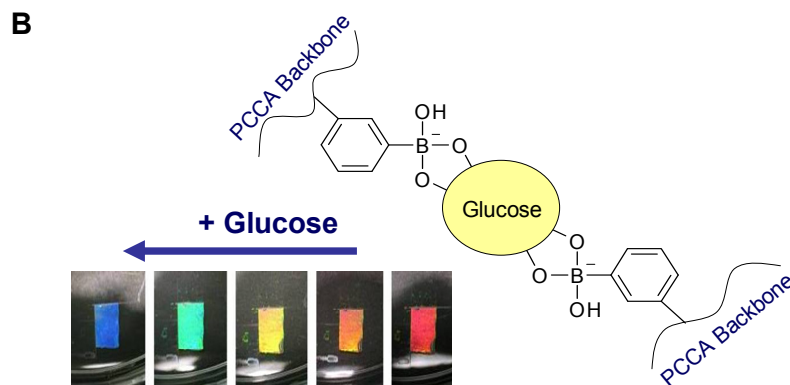
Figure 1-7. (A) The osmotic pressure resulting from changes in the free energy of elasticity derives from additional crosslinks formed upon analyte binding (c_{B2G}). (B) The glucose sensor utilizes boronic acid recognition molecules tethered to the PCCA hydrogel backbone, which are capable of forming 2:1 boronate:glucose sandwich complexes. Upon binding glucose, additional crosslinks are formed within the hydrogel network, shrinking the hydrogel volume and blue-shifting the diffraction wavelength.

The Donnan potential induced osmotic pressure arises due to a concentration gradient between mobile ions within and outside of the hydrogel matrix (Figure 1-8A)[1,2]. An example of an IPCCA that responds to changes in the free energy associated with ionic interactions is the lead sensor (Figure 1-8B)[42]. This IPCCA utilizes a crown ether that binds Pb^{+2}, resulting in this charged species and it's associated counter-ion being immobilized within the hydrogel. In low ionic strength solutions, this immobilization of charged groups within the hydrogel matrix causes a Donnan potential that swells the hydrogel and red-shifts the diffraction in proportion to the concentration of ions bound.

A

$$\Pi_{Ion} = RT(c_+ + c_- - c_+^* - c_-^*)$$

B

Pb^{+2}

Pendant Crown Ether
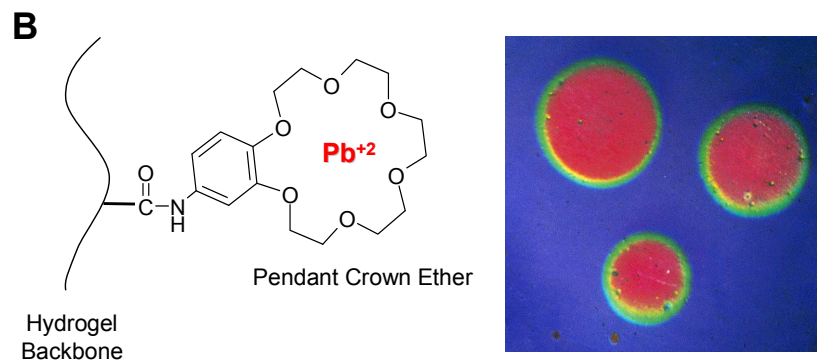
Hydrogel
Backbone

Figure 1-8. (A) The Donnan potential induced osmotic pressure arises due to a concentration gradient between mobile ions within and outside of the hydrogel matrix. (B) The lead sensor utilizes a crown ether that binds Pb^{+2}, resulting in this charged species and it's associated counter-ion being immobilized within the hydrogel. In low ionic strength solutions, this immobilization of charged groups within the hydrogel matrix causes a Donnan potential that swells the hydrogel and red-shifts the diffraction in proportion to the concentration of ions bound. The photograph illustrates the diffraction response to 3 drops of a Pb^{+2} solution placed on the IPCCA.

1.4   OVERVIEW OF RESEARCH PROGRAM

The work reported herein discusses the advances made in material development of responsive photonic crystal hydrogels.

Chapter 2 describes a new hydrogel system for the preparation of responsive PCCA based on the biocompatible and rehydratable polymer polyvinyl alcohol (PVA)[68]. We developed a new photonic crystal hydrogel material based on PVA, which can be reversibly dehydrated and

rehydrated, without the use of additional fillers, while retaining the diffraction and swelling properties of polymerized crystalline colloidal arrays. This chemically modified PVA hydrogel photonic crystal efficiently diffracts light from the embedded crystalline colloidal array. This diffraction optically reports on volume changes occurring in the hydrogel by shifts in the wavelength of the diffracted light. We fabricated a pH sensor, which demonstrates a 350 nm wavelength shift between pH values of 3.3 and 8.5. We have also fabricated a Pb^{+2} sensor, in which pendant crown ether groups bind lead ions. Immobilization of the ions within the hydrogel increases the osmotic pressure due to the formation of a Donnan potential, swelling the hydrogel and shifting the observed diffraction in proportion to the concentration of bound ions. The sensing responses of rehydrated PVA pH and Pb^{+2} sensors were similar to that before drying. This reversibility of rehydration enables storage of these hydrogel photonic crystal sensors in the dry state, which makes them much more useful for commercial applications.

Chapter 3 describes the advancements made towards developing photonic crystal glucose sensing materials to continuously monitor relatively high glucose concentrations, such as found in blood. We modified our synthetic fabrication methodologies in order to increase the glucose concentration range and to increase the reproducibility of our PCCA fabrication. We have also advanced our understanding of the sensing response by developing a mechanical method to independently determine the hydrogel crosslink density. Our investigation of the sensing mechanism indicates that binding depends mainly on the boronic acid concentrations and affinities, and we have determined the binding constant of 2-fluoro-5-aminophenyl boronic acid for glucose under physiological conditions. We have examined the dependence of glucose sensing upon interferences by other species that ligand to boronic acids such as lactate, as well as, human serum albumin. We examined the stability of our sensors over a period of weeks at

12

room temperature and demonstrated that we could further stabilize our sensing materials by reversibly dehydrating it for storage.

Chapter 4 describes the characterization of the mechanical properties of PCCA based on alterations in embedded CCA size and prepolymerization conditions. We experimentally determined the dependence of the elastic shear storage modulus for our photonic crystal hydrogels on their incorporated nanoparticle size and polymerization conditions. These hydrogels embed crystalline colloidal arrays of non-close-packed, monodisperse polystyrene particles. The modulus increases linearly with increasing polystyrene particle diameters between 114 nm and 186 nm. This dependence of the modulus on particle diameter results from interaction between the embedded nanoparticles and the hydrogel matrix, which involves slippage of the hydrogel at the particle surfaces due to the lack of adhesion. We also find that the shear storage moduli of hydrogels polymerized in the absence of oxygen are significantly larger than those polymerized in the presence of oxygen, and that this modulus difference is more pronounced for hydrogels prepared in the absence of the polystyrene crystalline colloidal arrays. The effective hydrogel crosslink densities can be determined from these storage modulus values. We can affect the responsivity of our photonic crystal materials by controlling the included nanoparticle size.

Chapter 5 provides a summary of each of the projects. We also provide suggestions for future work involving optimization and application.

1.5   REFERENCES

(1)   Erman, B.; Mark, J. E. *Structures and Properties of Rubberlike Networks*, Oxford University Press: New York, 1997.

(2)   Flory, P. J. *Principles of Polymer Chemistry*, Cornell University Press: New York, 1953.

(3)   Peppas, N. A.; Editor *Hydrogels in Medicine and Pharmacy, Vol. 3: Properties and Applications*, CRC Press: Boca Raton, 1987.

(4)   Peppas, N.; Editor *Hydrogels in Medicine and Pharmacy, Vol. I: Fundamentals*, CRC Press: Boca Raton, 1986.

(5)   Peppas, N. A.; Editor *Hydrogels in Medicine and Pharmacy, Vol. II: Polymers*, CRC Press: Boca Raton, 1987.

(6)   Nguyen, K. T.; West, J. L. *Biomaterials* **2002**, *23*, 4307-4314.

(7)   Ifkovits, J. L.; Burdick, J. A. *Tissue Eng.* **2007**, *13*, 2369-2385.

(8)   Nuttelman, C. R.; Rice, M. A.; Rydholm, A. E.; Salinas, C. N.; Shah, D. N.; Anseth, K. S. *Prog. Polym. Sci.* **2008**, *33*, 167-179.

(9)   Peppas, N. A.; Bures, P.; Leobandung, W.; Ichikawa, H. *Eur. J. Pharm. Biopharm.* **2000**, *50*, 27-46.

(10)   Alvarez-Lorenzo, C.; Concheiro, A. *Mini-Rev. Med. Chem.* **2008**, *8*, 1065-1074.

(11)   Liu, X.; Nakamura, K.; Lowman, A. M. *Soft Mater.* **2003**, *1*, 393-408.

(12)   Kim, J. J.; Park, K. *Bioseparation* **1998**, *7*, 177-184.

(13)   Wang, K. L.; Burban, J. H.; Cussler, E. L. *Adv. Polym. Sci.* **1993**, *110*, 67-79.

(14)   Haney Paul, J.; Draveling, C.; Durski, W.; Romanowich, K.; Qoronfleh, M. W. *Protein Expr. Purif.* **2003**, *28*, 270-279.

(15)   Galaev, I. Y.; Mattiasson, B. *Enzyme Microb. Technol.* **1993**, *15*, 354-366.

(16) Hyon, S. H.; Cha, W. I.; Ikada, Y.; Kita, M.; Ogura, Y.; Honda, Y. *J. Biomat. Sci.-Polym. E.* **1994**, *5*, 397-406.

(17) Buhler, N.; Haerri, H. P.; Hofmann, M.; Irrgang, C.; Muhlebach, A.; Muller, B.; Stockinger, F. *Chimia* **1999**, *53*, 269-274.

(18) Chaterji, S.; Kwon, I. K.; Park, K. *Prog. Polym. Sci.* **2007**, *32*, 1083-1122.

(19) Krsko, P.; Libera, M. *Mater. Today* **2005**, *8*, 36-44.

(20) Mano, J. F. *Adv. Eng. Mater.* **2008**, *10*, 515-527.

(21) Kopecek, J.; Yang, J. Y. *Polym. Int.* **2007**, *56*, 1078-1098.

(22) Peppas, N. A.; Hilt, J. Z.; Khademhosseini, A.; Langer, R. *Adv. Mater.* **2006**, *18*, 1345-1360.

(23) van der Linden, H. J.; Herber, S.; Olthuis, W.; Bergveld, P. *Analyst* **2003**, *128*, 325-331.

(24) Roy, I.; Gupta, M. N. *Chem. Biol.* **2003**, *10*, 1161-1171.

(25) Yoshida, R. *Curr. Org. Chem.* **2005**, *9*, 1617-1641.

(26) Gil, E. S.; Hudson, S. A. *Prog. Polym. Sci.* **2004**, *29*, 1173-1222.

(27) Li, Y.; Tanaka, T. *Annu. Rev. Mater. Sci.* **1992**, *22*, 243-277.

(28) Richter, A.; Paschew, G.; Klatt, S.; Lienig, J.; Arndt, K.-F.; Adler, H.-J. P. *Sensors* **2008**, *8*, 561-581.

(29) Gupta, P.; Vermani, K.; Garg, S. *Drug Discov. Today* **2002**, *7*, 569-579.

(30) Prabaharan, M.; Mano, J. F. *Macromol. Biosci.* **2006**, *6*, 991-1008.

(31) Klouda, L.; Mikos, A. G. *Eur. J. Pharm. Biopharm.* **2008**, *68*, 34-45.

(32) Zeng, X.; Jiang, H. *Appl. Phys. Lett.* **2008**, *93*, 151101/151101-151101/151103.

(33) Sako, Y.; Takaguchi, Y. *Org. Biomol. Chem.* **2008**, *6*, 3843-3847.

(34) Satarkar, N. S.; Hilt, J. Z. *J. Controlled Release* **2008**, *130*, 246-251.

(35) Hu, S.-H.; Liu, T.-Y.; Liu, D.-M.; Chen, S.-Y. *Macromolecules* **2007**, *40*, 6786-6788.

(36) Xu, X.; Majetich, S. A.; Asher, S. A. *J. Am. Chem. Soc.* **2002**, *124*, 13864-13868.

(37) Maurer, M. K.; Lednev, I. K.; Asher, S. A. *Adv. Funct. Mater.* **2005**, *15*, 1401-1406.

(38) Lee, K.; Asher, S. A. *J. Am. Chem. Soc.* **2000**, *122*, 9534-9537.

(39) Walker, J. P.; Kimble, K. W.; Asher, S. A. *Anal. Bioanal. Chem.* **2007**, *389*, 2115-2124.

(40) Sunkara, H. B.; Weissman, J. M.; Penn, B. G.; Frazier, D. O.; Asher, S. A. *Polym. Prepr.* **1996**, *37*, 453-454.

(41) Sharma, A. C.; Jana, T.; Kesavamoorthy, R.; Shi, L.; Virji, M. A.; Finegold, D. N.; Asher, S. A. *J. Am. Chem. Soc.* **2004**, *126*, 2971-2977.

(42) Reese, C. E.; Asher, S. A. *Anal. Chem.* **2003**, *75*, 3915-3918.

(43) Holtz, J. H.; Holtz, J. S. W.; Munro, C. H.; Asher, S. A. *Anal. Chem.* **1998**, *70*, 780-791.

(44) Holtz, J. H.; Asher, S. A. *Nature* **1997**, *389*, 829-832.

(45) Baca, J. T.; Finegold, D. N.; Asher, S. A. *Analyst* **2008**, *133*, 385-390.

(46) Asher, S. A.; Sharma, A. C.; Goponenko, A. V.; Ward, M. M. *Anal. Chem.* **2003**, *75*, 1676-1683.

(47) Alexeev, V. L.; Das, S.; Finegold, D. N.; Asher, S. A. *Clin. Chem.* **2004**, *50*, 2353-2360.

(48) Asher, S. A.; Holtz, J. H.: US Patent 5854078, 1998.

(49) Asher, S. A.; Holtz, J. H.: WO Patent 9819787, 1998.

(50) Asher, S. A.; Holtz, J. H.: WO Patent 9841859, 1998.

(51) Asher, S. A.; Holtz, J.; Liu, L.; Wu, Z. *J. Am. Chem. Soc.* **1994**, *116*, 4997-4998.

(52) Tikhonov, A.; Coalson, R. D.; Asher, S. A. *Phys. Rev. B: Condens. Matt. Mater. Phys.* **2008**, *77*, 235404/235401-235404/235416.

(53)   Asher, S. A.; Weissman, J. M.; Tikhonov, A.; Coalson, R. D.; Kesavamoorthy, R. *Phys. Rev. E: Stat., Nonlinear, Soft Matter Phys.* **2004**, *69*, 066619/066611-066619/066614.

(54)   Reese, C. E.; Guerrero, C. D.; Weissman, J. M.; Lee, K.; Asher, S. A. *J. Colloid Interface Sci.* **2000**, *232*, 76-80.

(55)   Asher, S. A.; Holtz, J.; Weissman, J.; Pan, G. *MRS Bulletin* **1998**, *23*, 44-50.

(56)   Asher, S. A.: EP Patent 168988, 1986.

(57)   Flaugh, P. L.; O'Donnell, S. E.; Asher, S. A. *Appl. Spectrosc.* **1984**, *38*, 847-850.

(58)   Carlson, R. J.; Asher, S. A. *Appl. Spectrosc.* **1984**, *38*, 297-304.

(59)   Rundquist, P. A.; Photinos, P.; Jagannathan, S.; Asher, S. A. *J. Chem. Phys.* **1989**, *91*, 4932-4941.

(60)   Alexeev, V. L.; Sharma, A. C.; Goponenko, A. V.; Das, S.; Lednev, I. K.; Wilcox, C. S.; Finegold, D. N.; Asher, S. A. *Anal. Chem.* **2003**, *75*, 2316-2323.

(61)   Ben-Moshe, M.; Alexeev, V. L.; Asher, S. A. *Anal. Chem.* **2006**, *78*, 5149-5157.

(62)   Asher, S. A.; Alexeev, V. L.; Goponenko, A. V.; Sharma, A. C.; Lednev, I. K.; Wilcox, C. S.; Finegold, D. N. *J. Am. Chem. Soc.* **2003**, *125*, 3322-3329.

(63)   Asher, S. A.; Alexeev, V. L.; Lednev, I. K.; Sharma, A. C.; Wilcox, C.: US Patent 2003027240, 2003.

(64)   Asher, S. A.; Peteu, S. F.; Reese, C. E.; Lin, M. X.; Finegold, D. *Anal. Bioanal. Chem.* **2002**, *373*, 632-638.

(65)   Kimble, K. W.; Walker, J. P.; Finegold, D. N.; Asher, S. A. *Anal. Bioanal. Chem.* **2006**, *385*, 678-685.

(66)   Xu, X.; Goponenko, A. V.; Asher, S. A. *J. Am. Chem. Soc.* **2008**, *130*, 3113-3119.

(67)   Walker, J. P.; Asher, S. A. *Anal. Chem.* **2005**, *77*, 1596-1600.

(68)   Muscatello, M. M. W.; Asher, S. A. *Adv. Funct. Mater.* **2008**, *18*, 1186-1193.

2.0 POLY VINYL ALCOHOL REHYDRATABLE PHOTONIC CRYSTAL SENSOR MATERIALS

We developed a new photonic crystal hydrogel material based on the biocompatible polymer poly (vinyl alcohol) (PVA), which can be reversibly dehydrated and rehydrated, without the use of additional fillers, while retaining the diffraction and swelling properties of polymerized crystalline colloidal arrays (PCCA). This chemically modified PVA hydrogel photonic crystal efficiently diffracts light from the embedded crystalline colloidal array. This diffraction optically reports on volume changes occurring in the hydrogel by shifts in the wavelength of the diffracted light. We fabricated a pH sensor, which demonstrates a 350 nm wavelength shift between pH values of 3.3 and 8.5. We have also fabricated a Pb^{+2} sensor, in which pendant crown ether groups bind lead ions. Immobilization of the ions within the hydrogel increases the osmotic pressure due to the formation of a Donnan potential, swelling the hydrogel and shifting the observed diffraction in proportion to the concentration of bound ions. The sensing responses of rehydrated PVA pH and Pb^{+2} sensors were similar to that before drying. This reversibility of rehydration enables storage of these hydrogel photonic crystal sensors in the dry state, which makes them much more useful for commercial applications.

2.1   INTRODUCTION

Poly(vinyl alcohol) (PVA) is a polymer that is already extensively utilized in industrial and biomedical applications, owing largely to its mechanical properties and biocompatibility.[1-6] PVA hydrogels have been used or are being investigated for use in many biomedical applications, such as drug delivery,[7-9] intervertebrate discs,[10,11] contact lenses,[12,13] articular cartilage,[14,15] and wound dressing.[16,17] The properties, and thereby possible applications, of PVA hydrogels can be tailored by manipulating the type and concentration of crosslinks within the material.

PVA hydrogels can be formed utilizing using either physical or chemical crosslinking. There have been extensive studies of PVA hydrogels that contain crystalline regions, which act as physical crosslinks, which are created by repetitive freeze-thaw cycles.[4,18-26] Although these hydrogels are stable at room temperature for months, these physical crosslinks are less mechanically and thermally stable than are chemical crosslinks.

Traditionally, one of the most widely used methods for preparing chemically crosslinked PVA hydrogels utilized glutaradehyde as a crosslinker.[27-31] However, due to the cytotoxic nature of glutaradehyde[32-35] several groups have prepared chemically crosslinked PVA hydrogels utilizing other crosslinkers such as epichlorohydrin,[36] diglycidyls,[37] or by incorporation of polymerizeable functionalities[38-43] onto the PVA backbone.

We report here the fabrication of a novel and inexpensive photonic crystal hydrogel sensing material prepared from modified poly (vinyl alcohol), which is based on our previously developed photonic crystal materials.[44-51] These materials utilize a mesoscopically periodic array of colloidal particles that self-assembles into a highly-ordered crystalline colloidal array (CCA)

20

(Figure 2-1A). The lattice spacing of the CCA is fabricated such that visible light is Bragg diffracted.

When the CCA is polymerized within a hydrogel (PCCA) (Figure 2-1B), it optically reports on volume changes experienced by the material, since the observed diffraction wavelength is directly related to the spacing between lattice planes.[47,52-64] To apply this motif to chemical sensing, the hydrogel is functionalized such that it responds to changes in the analyte concentration by altering its volume and diffraction wavelength.[52,53,55,56,65-81] Previously developed PCCA hydrogels have utilized acrylamide,[52] methylacrylate,[61] poly (ethylene glycol) acrylates,[62,64] and N-isopropylacrylamide.[63]

We demonstrated three primary mechanisms of PCCA photonic crystal sensing, employing changes in the hydrogel crosslink density, immobilization of ions on the hydrogel, or changes in the free energy of mixing of the hydrogel polymer with the aqueous medium. In the crosslinking archetype, the analyte molecule is bound by two molecular recognition molecules, which are tethered to the hydrogel, forming additional crosslinks within the hydrogel causing it to shrink. The consequential decrease in the particle array lattice constant blue-shifts the wavelength of light diffracted by the PCCA as the crosslink density increases. This motif was previously demonstrated for sensing of glucose,[66,69,74] metal ions such as Cu^{+2},[72] and ammonia.[65] The second sensing motif employs the immobilization of ions within the hydrogel, increasing the osmotic pressure and swelling the hydrogel. The resulting increase in the particle array lattice constant red-shifts the wavelength of diffracted light as the concentration of bound charges increases. This motif has been demonstrated for sensing of Pb^{+2},[53,56,70,75,76] glucose,[53,56] pH,[55,76] and organophosphates.[67] In the third sensing motif, the balance between the free energy of mixing of the hydrogel polymer with the surrounding medium and the elastic restoring force of

21

the hydrogel crosslinks determines the PCCA hydrogel volume. Alterations to the hydrogel polymer that result in an increase in the polymer solubility make the free energy of mixing more favorable, thereby swelling the hydrogel and red-shifting the diffraction wavelength. This motif was previously demonstrated for photochemically controlled photonic crystal materials[82-85] and utilized with the sensing of creatinine.[68]
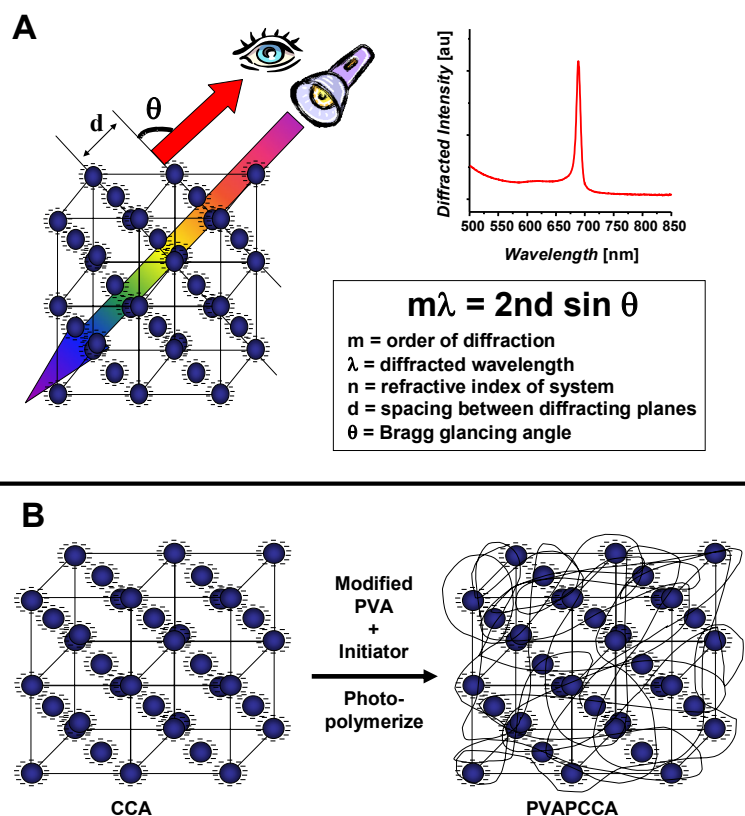
Figure 2-1. (A) Crystalline Colloidal Arrays (CCA) form due to the electrostatic repulsion between the highly charged, monodisperse polystyrene particles. The spacing between particles is such that they diffract visible light according to Bragg's law. (B) Polymerized Crystalline Colloidal Arrays (PCCA) are formed by polymerizing a hydrogel network around the CCA.

This new PVA photonic crystal hydrogel material efficiently Bragg diffracts light and can be reversibly dried and rehydrated, without the use of fillers, while retaining the original diffraction and swelling properties. We fabricated polyvinyl alcohol PCCA (PVAPCCA) sensors for determining pH and Pb^{+2} and compared the sensor response prior to and after drying and rehydrating the material. The response of these new PVAPCCA sensors is comparable to our previously developed sensors;[53,55,56,76] however, the reversible hydration property of this new material affords for more practical storage and transport.

2.2   RESULTS AND DISCUSSION

We previously fabricated acrylamide-based PCCA, which demonstrated volume-phase transitions and diffraction changes in response to variations in pH and ionic strength.[55,76] We also previously fabricated acrylamide-based PCCA lead sensors, which utilized pendant crown ether groups to bind Pb^{+2}.[49,53,56,70,75,76] The sensing capabilities of both of these hydrogel sensors relied on the formation of ionic hydrogels,[86-89] either by direct incorporation of charged groups via partial hydrolysis of amide groups by the formation of titratable carboxyls or by use of chelating agents to bind charged groups to the hydrogel. As the bound charge on the hydrogels increases, there is an immobilization of counterions within the hydrogel, which increases the osmotic pressure, thereby swelling the hydrogel against the restoring elasticity. This swelling red-shifts the diffracted wavelength. This red-shift continues until all carboxyl groups are deprotonated or all crown ethers are complexed to Pb^{+2}, after which further increases in pH or additional lead concentration merely increase the ionic strength such that the osmotic pressure is decreased, shrinking the hydrogel and blue-shifting the diffracted light wavelength.

23

Figure 2-2 illustrates the pH and ionic strength diffraction dependence of an ionic PVA-based pH sensing hydrogel, which was prepared by reacting a PVAPCCA with succinic anhydride in DMSO for 1.5 hours. As illustrated, the diffraction monotonically red-shifts over ~350 nm for pH values between 3.3 and 8.5 as pendant carboxyl groups are ionized, and then blue-shifts for higher pH values as the ionic strength increases. This response is similar to that observed previously by Lee et al,[55] but differs from the recently observed hysteresis response of pH sensitive PCCA prepared by Xu et al,[90] where the PCCA was first equilibrated at either a low or high pH and then titrated by adding either NaOH or HCl.
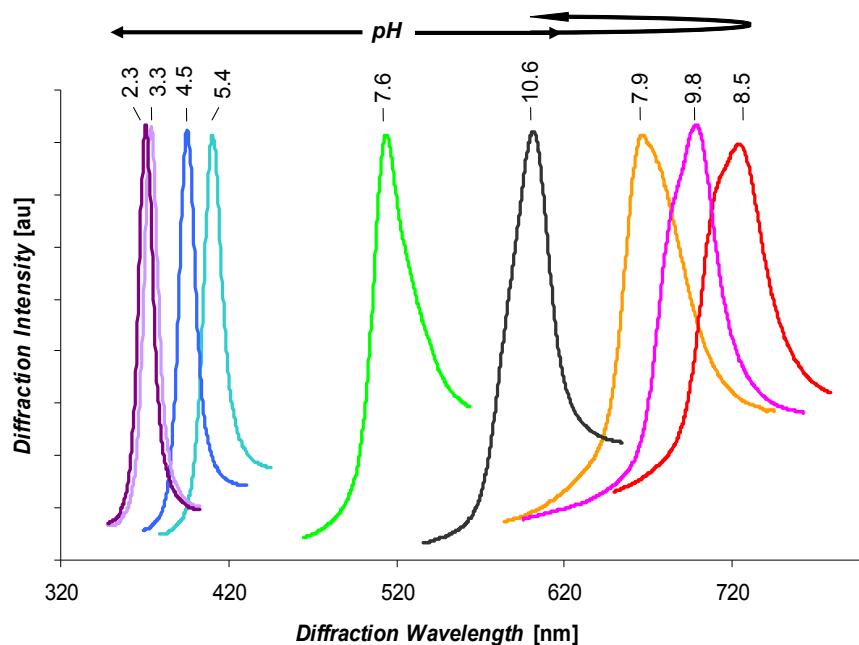
Figure 2-2. The diffraction dependence of an ionic PVAPCCA, prepared by coupling with succinic anhydride in DMSO for 1.5 hours, on changes in pH and ionic strength. The diffraction monotonically redshifts for pH values increasing from pH 2 to pH 9 as pendant carboxyl groups are ionized. Blue-shifts occur for higher pH values as the ionic strength increases.

Although the response of this pH sensor is akin to previously developed pH sensors, a significant difference between this PVAPCCA pH sensor and previously developed PCCA pH sensors is its ability to be dehydrated and rehydrated while retaining the CCA ordering and the sensing capability of the hydrogel. Figure 2-3 compares the diffraction response to changes in pH experienced by the same PVAPCCA hydrogel, prior to drying and after rehydration. As can be seen in Figure 2-4, the swelling ability and diffraction of the material is preserved, even upon drying.
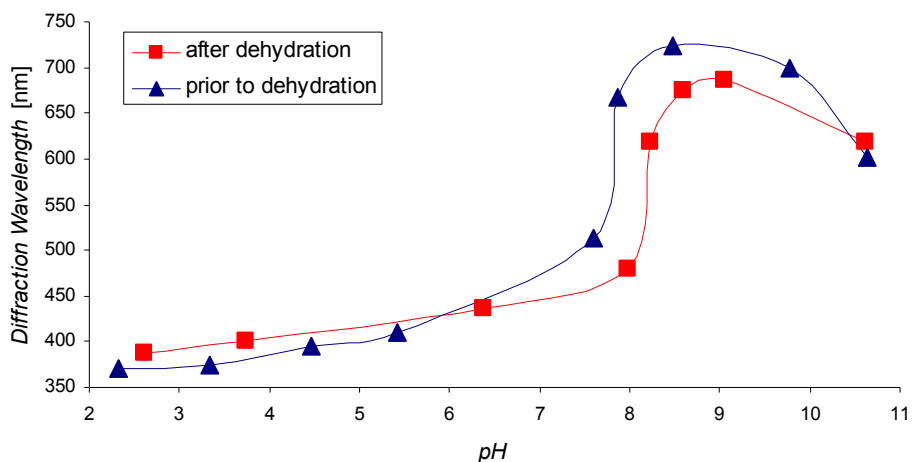
Figure 2-3. Comparison of diffraction response from ionic PVAPCCA to changes in pH values prior to drying (blue) and after rehydration (red). (Lines added to aid the eye.) Determining the reality of measured diffraction wavelength differences between the dehydrated and original sample has to take cognizance of the fact that the spectrometer precision is ±1 nm and the sample inhomogeneity across the surface is ±5 nm. The major uncertainty in this figure is the variability in the measured pH of pure water between the values of pH=5 to pH=9, which shows variability of almost ±1.5 pH units. The increased ionic strength outside this range results in reliable pH values.

25
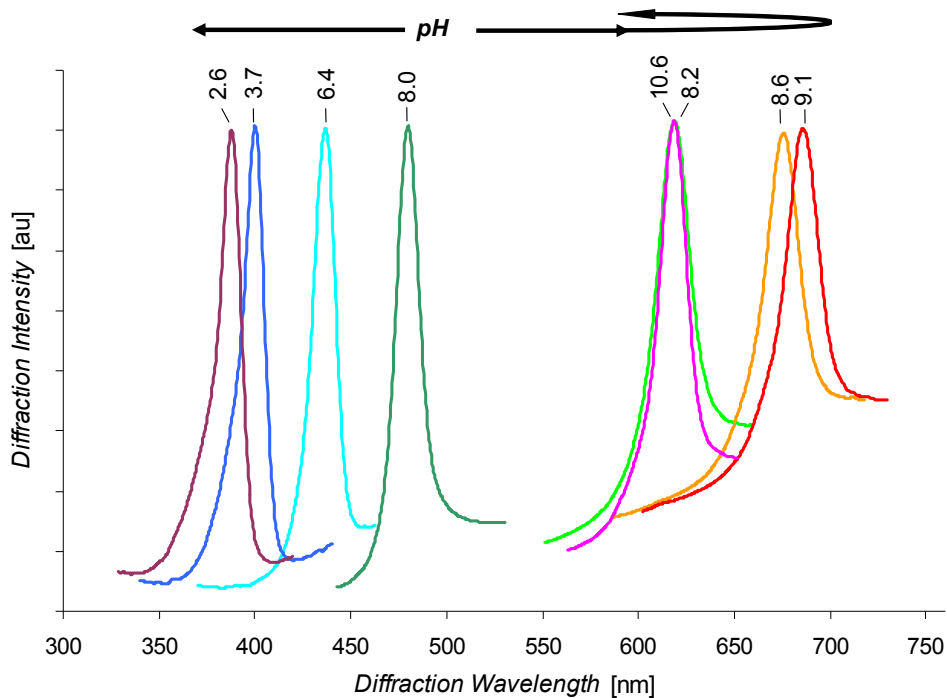
Figure 2-4. The diffraction dependence of an ionic PVAPCCA, after rehydration, on changes in pH and ionic strength. The material retains swelling and diffraction properties even after drying.

Determining the reality of measured diffraction wavelength differences between the dehydrated and original sample has to take cognizance of the fact that the spectrometer precision is ±1 nm and the sample inhomogeneity across the surface is ±5 nm. The major uncertainty in this figure is the variability in the measured pH of pure water between the values of pH=5 to pH=9, which shows variability of almost ±1.5 pH units. The increased ionic strength outside this range results in reliable pH values.

Figure 2-5 illustrates the diffraction dependence of the PVAPCCA, which contains pendant crown ether groups, to changes in solution Pb^{+2} concentration prior to drying in vacuum and after rehydration. As in the previously developed acrylamide-based lead sensors, when Pb^{+2} is bound by the pendant crown ether groups there is an increased osmotic pressure, which swells

the hydrogel, and red-shifts the diffraction. Unlike the previously developed acrylamide-based sensor, this PVAPCCA exhibits efficient diffraction upon rehydration, as illustrated by the relatively narrow reflection peak of the rehydrated hydrogel in Figure 2-6. Clearly, PVA hydrogels maintain CCA order upon drying.
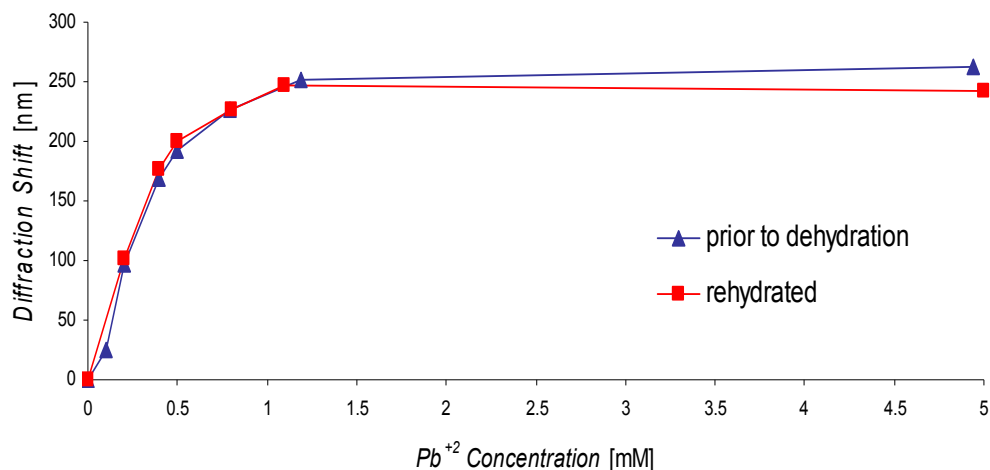
Figure 2-5. The diffraction dependence of a PVAPCCA containing crown ethers on Pb^{+2} concentration prior to dehydration (blue) and after rehydration (red). (Lines added to aid the eye.) Determining the reality of measured diffraction wavelength differences between the dehydrated and original sample has to take into consideration the spectrometer precision (± 1 nm) and the sample inhomogeneity across the surface (± 5 nm).

The majority of variation in the observed absolute diffraction wavelength for the original and rehydrated PVCPCCA, as illustrated in Figure 2-6, could be derived from several factors, including diffraction inhomogeneity (± 5 nm) across the surface of a PCCA, and the different affixation of the hydrogel to the substrate. The diffraction measurements prior to dehydration were taken from the PVAPCCA originally affixed to the quartz plate during polymerization. The diffraction measurements after rehydration were taken from the hydrogel after it was

released from the quartz plate, dried, rehydrated, and reattached to a Petri dish. Release of the PVAPCCA from the quartz plate results in a diffraction blue-shift because the hydrogel is no longer constrained to swelling in only one dimension. As illustrated in Figure 2-5, comparison of the diffraction shift in response to changes in analyte concentration, which is an indicator of the hydrogel's mechanical properties, clearly shows that the sensing ability of the PVAPCCA remains nearly unchanged even after drying in vacuum.
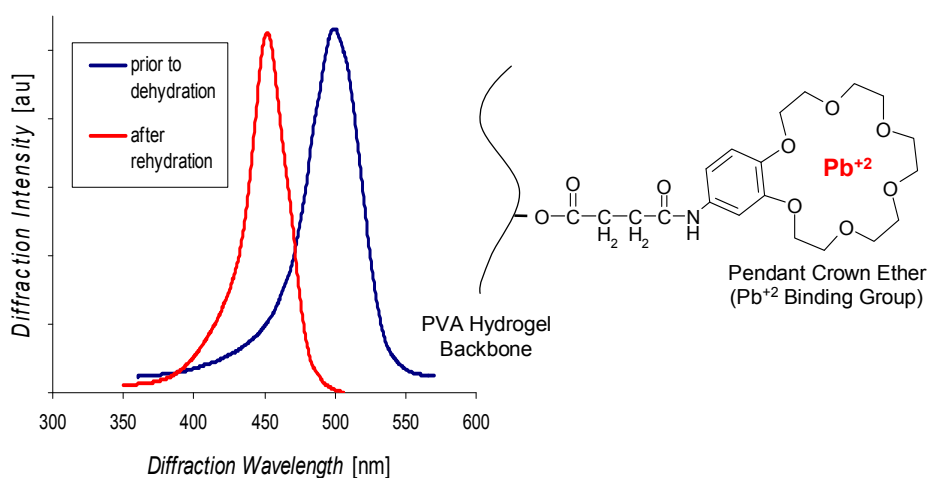
Figure 2-6. As Pb^{+2} is bound by the pendant crown ether groups, there is an increased osmotic pressure, swelling the hydrogel, and red-shifting the diffraction. Although the diffraction wavelength shift is nearly identical, the rehydrated sensor shows a ~50 nm blue-shift in absolute diffraction (both peaks measured at 0.4 mM Pb^{+2}).

Previously developed acrylamide-based PCCA disorder upon dehydration. These PCCA do not, in general, regain diffraction after rehydration due to irreversible changes in morphology and collapse of the hydrogel. However, we recently observed the reversible dehydration and rehydration of an acrylamide-based PCCA Ni^{+2} sensing material, in the case where the PCCA

was covalently attached to a gel support film and dried in the presence of buffer, which served as a stabilizer as the solution concentrated upon drying.[91]

Ceylan et al studied the deswelling in acetone and the reswelling in water of a series of ionic poly (acrylamide) hydrogels[92] and noted that acrylamide hydrogels do not regain their initial volume after collapse in acetone. Allen et al disclosed a method to prepare rehydratable polyacrylamide hydrogels for use in electrophoresis that could be stored dry for extended periods of time at ambient temperatures and rehydrated without loss of structural or functional integrity.[93,94] These hydrogels incorporated polyols, polymeric alcohols, polyamines or high molecular weight polysaccharides such as dextran or substituted monosaccharides as stabilizers, to prevent irreversible damage to the gel matrix structure upon dehydration. Even though these hydrogels could be reswelled to 80-95% of their original volume, depending on the stabilizer used, it was preferred that they be stored in controlled humidity sealed containers since the hydrogel pore spaces could collapse if the relative humidity decreased below 70%.

PVA, on the other hand, is known to be a readily rehydratable polymer. Ricciardi et al recently demonstrated that PVA hydrogels, lacking additives or stabilizers, exhibit physical properties upon rehydration comparable to those before dehydration.[24,25] As our PVAPCCA Bragg diffracts light from the 111 plane of the embedded CCA that is aligned parallel to the hydrogel surface and we observe the back-diffraction of incident light normal to the hydrogel surface, the back-diffracted wavelength (λ) depends on the 111 plane spacing (d) and the refractive index of the system (n): $\lambda=2nd$.

Since changes in the PVAPCCA hydrogel volume give rise to changes in the diffracted wavelength, and given that d is proportional to the third root of the volume, the change in hydrogel volume can be easily determined:

$$\frac{\lambda}{\lambda'} = \left(\frac{V}{V'}\right)^{\frac{1}{3}}$$

Equation 2-1

where λ is the diffraction wavelength of the rehydrated hydrogel and λ' is the diffraction wavelength prior to dehydration.

We typically observe a 30-35 nm blue-shift in the diffraction wavelength upon removing the PCCA from its substrate. Figure 2-5 indicates a ~50 nm diffraction difference prior to versus after rehydration.   This net 20 nm blue-shift suggests that our dehydrated crown ether PVAPCCA material reswells to ~90% of the initial volume after drying in vacuum.   The recovered hydrogel maintains its sensing response, even after drying in vacuum, without the use of any filler molecules.

Successful sensor development requires the development of sensing materials with significant shelf lives at room temperature, and extended lifetimes with refrigeration or freezing. A major factor in sensor lifetime is the stability of the incorporated molecular recognition molecule, which depends on the ambient conditions inside the hydrogel, such as pH and temperature, or the immobilization itself. Recently, researchers have shown that immobilization of a molecular recognition elements, such as enzymes, to or within a support matrix significantly increases the enzyme activity lifetime.[95-97] The ability of our PVAPCCA hydrogel material to dehydrate and reversibly rehydrate enables this technology to utilize unstable molecular recognition elements and increases its potential for commercial applications.

2.3   CONCLUSIONS

We developed a new composition of a photonic crystal hydrogel materials based on chemically modified poly (vinyl alcohol). The vinyl groups attached to the PVA can be used to crosslink the polymer, eliminating the necessity of an additional crosslinker. This PVAPCCA efficiently diffracts visible light and reports on volume transitions experienced by the hydrogel by shifting the diffracted wavelength. This photonic crystal can be utilized for the determination of pH, Pb^{+2}, and, with the use of additional recognition elements, other analytes. Most notably this material can be dried and then rehydrated by immersion in water, while retaining its diffraction and mechanical properties. This reversibility of rehydration affords storage of hydrogel sensors in the dry state, facilitating their commercialization.

2.4   EXPERIMENTAL

2.4.1   Materials

Pyridine, $Pb(NO_3)_2$, NaOH, and KCl were purchased from Sigma. Succinic anhydride was purchased from Aldrich. Hydroquinone-monomethyl ether (HQME), glycidyl methacrylate (GMA), and 4′-Aminobenzo-18-crown-6 (18C6) were purchased from Fluka. Dimethyl sulfoxide (DMSO) and HCl were purchased from Fisher Scientific. Poly (vinyl alcohol) 88 mol% hydrolyzed, MW~25kDa (PVA) was purchased from Polysciences, Inc. Acetone was purchased from EMD Chemicals, Inc. 2,2-diethoxyacetophenone (DEAP) was purchased from Acros Organics. Ethanol (EtOH) was purchased from Pharmco Products, Inc. Phosphate

Buffered Saline (0.1 M phosphate, 0.15 M NaCl, pH 7.2, PBS), and 1-ethyl-3-(3-dimethylaminopropyl) carbodiimide hydrochloride (EDC) were purchased from Pierce Biotechnology. All chemicals were used as received.

2.4.2 Modification of Poly(vinyl alcohol) with Glycidyl Methacrylate

Partially hydrolyzed PVA was functionalized with methacrylate groups by reaction with GMA in DMSO, as reported elsewhere[42,43] (Figure 2-7). In a typical synthesis HQME (0.35g) inhibitor, DMSO (100 mL), PVA (10 g), and pure water (5 mL) were added to a jacketed round-bottom flask. The flask was sealed, and the solution was purged with N_2 (30 min) and kept under a N_2 blanket while being stirred at 300 rpm for 1.5 - 2 hours at $80^{o}C$. GMA (70-90 mL) and HCl (4 mL) were added to the flask by a syringe. The temperature was lowered to 50 ^{o}C, and the reaction proceeded with constant stirring (300 rpm) under nitrogen overnight. The resulting solution was cooled to room temperature and precipitated into a large volume of acetone with vigorous stirring. The precipitate was collected via filtration. The precipitate was suspended in acetone (~100 mL, changed daily) with constant shaking for 5-7 days, then collected by filtration and dried in vacuum.

2.4.3 CCA Preparation

Monodisperse, highly-charged colloids were prepared via emulsion polymerization as previously described.[48] We used ~15% w/w suspensions of ~100 nm polystyrene sphere CCA dispersed in pure water. The colloidal particles were cleaned via dialysis against deionized pure

water and subsequently shaken with ion-exchange resin. Once sufficiently cleaned, the suspension became iridescent due to Bragg diffraction.
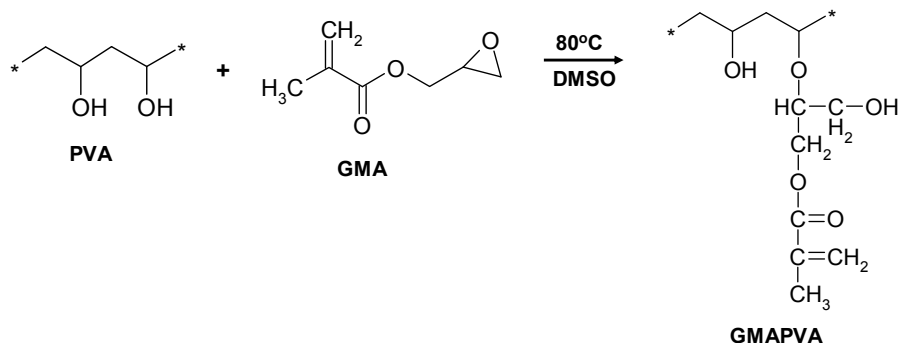
Figure 2-7. Poly (vinyl alcohol) (PVA) modified with a pendant methacrylate group by reaction of a small percent of hydroxyls with glycidyl methacrylate (GMA), resulting in a readily photopolymerizable monomer (GMAPVA).

2.4.4   PVAPCCA Hydrogel Preparation

Solutions (22 wt%) of the glycidyl methacrylate modified PVA (GMAPVA) were prepared by dissolving GMAPVA in pure water via heating the solution to near-boiling and vortexing. CCA (0.8 mL) and ion exchange resin were combined with the GMAPVA solution (0.4 mL) in a vial and vortexed. DEAP (10 μL, 20% in DMSO) was added to this solution. The solution was vortexed and then centrifuged for 5 minutes. The solution was polymerized, in a cell consisting of two quartz plates separated by a 125 μm parafilm spacer and exposed to UV light from two Blak Ray (365 nm) mercury lamps. The resulting PVAPCCA was removed from the cell and rinsed with large quantities of pure water.

2.4.5   PVAPCCA Hydrogel Carboxylation

The PVAPCCA was carboxylated by treatment with succinic anhydride in an anhydrous solvent, such as DMSO, (Figure 2-8).[37]   This was accomplished by first transferring the PVAPCCA to DMSO and allowing it to equilibrate.   The PVAPCCA was then placed in a solution of succinic anhydride in DMSO (0.1 g/mL), to which pyridine (0.6:1 succinic anhydride: pyridine) was added dropwise. The reaction proceeded in a 40 $^\circ$C water bath for 1.5 - 48 hours. The hydrogel was then rinsed with DMSO and copious amounts of pure water. The level of carboxylation of the hydrogel was controlled by the succinic anhydride concentration used and/or the reaction time.
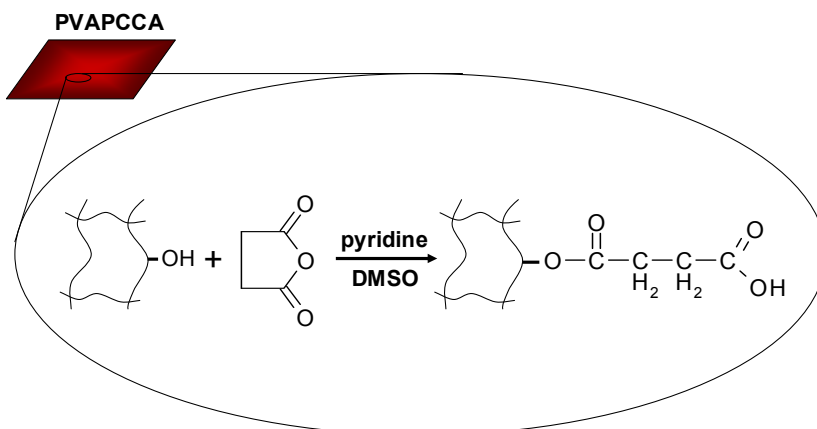
Figure 2-8. After polymerization of PVA, a fraction of the remaining hydroxyls were reacted with succinic anhydride to incorporate carboxyl groups onto the hydrogel backbone.

34

2.4.6   PVAPCCA Hydrogel Crown Ether Incoroporation

Incorporation of the crown ether into the hydrogel backbone was accomplished through carbodiimide coupling, utilizing a solution of 18C6 (20 mM) and EDC (25 mM). The reaction proceeded for 2 hours at room temperature, after which a second coupling reaction was completed to ensure complete coupling of crown ether to carboxyl groups. The hydrogel was rinsed extensively with pure water.

2.4.7   Dehydrating/Rehydrating of PVAPCCA

After characterizing the response of the diffraction of the PVAPCCA to changes in pH, ionic strength, or lead concentrations, the hydrogel sensors were dehydrated as a free film. The PVAPCCA in pure water was exchanged in EtOH. The hydrogel was then air dried, while maintaining gentle mechanical constraints to prevent curling, and then dried overnight under ambient conditions. The Pb^{+2} sensitive PVAPCCA was air dried and then further dried under vacuum for 2 hours. The dehydrated PVAPCCA was rehydrated by directly immersing it in pure water and equilibrating it at room temperature.

2.4.8   Characterization of GMAPVA

The extent of modification of the polyvinyl alcohol was determined by using ^{1}H-NMR (300 MHz, D_2O, 25°C). The vinyl protons were ratioed against the PVA backbone protons to calculate the percent modification. The extent of modification was varied from 0.5% to 5.5% by varying the amount of glycidyl methacrylate in the reaction mixture.

2.4.9   Diffraction Measurements

Diffraction measurements were conducted at a fixed 90° glancing angle utilizing an Ocean Optics USB2000-UV-VIS Spectrometer, a LS-1 Tungsten Halogen Light Source or a DT 1000 CE UV/VIS Light Source, and an R-series Fiber Optic Reflection Probe. The PVAPCCA to be characterized was affixed to a quartz plate or polystyrene petri dish, by the typical adhesion which occurs upon contact with the substrate, in order to fix the hydrogel's position throughout the diffraction measurements. Experiments were conducted in a covered petri dish, so as to avoid evaporation. Holes were drilled in the lid and were secured with parafilm, allowing access for the reflection probe and addition/removal of solutions.

To characterize the response of the PVAPCCA to changes in pH, the hydrogel was first equilibrated in pure water. Small volumes of dilute NaOH were added to the dish and the diffraction was monitored until it stabilized, at which time the pH of the water was sampled as described below and the diffraction wavelength was recorded. The titration with NaOH occurred until the diffraction red-shifting plateaued and began to blue-shift. The PVAPCCA was then rinsed with copious amounts of pure water and the process was repeated by using small increments of dilute HCl to lower the pH. HCl was added until the diffraction blue-shifting plateaued.

To characterize the response of the crown ether PVAPCCA to Pb^{+2}, the hydrogel was first equilibrated in pure water. Small increments of concentrated $Pb(NO_3)_2$ were added to the dish and the diffraction was monitored until it stabilized, at which time the diffraction wavelength was recorded. Pb^{+2} was added until the diffraction red-shifting plateaued.

2.4.10 pH Measurements

pH measurements were conducted by first collecting ~15 mL of water from the petri dish containing the PVAPCCA after the hydrogel had equilibrated and then replacing this sample with fresh nanopure water prior to additional adjustments in solution pH so as to maintain a constant volume. The ionic strength of the sampled water was increased by adding a small volume of concentrated KCl, resulting in a 150 mM KCl solution, thereby reducing noise and improving the accuracy and reproducibility of measuring the pH of water.

2.5   ACKNOWLEDGEMENTS

2.6   REFERENCES

(1)   C. A. Finch, *Polyvinyl Alcohol*, John Wiley & Sons: London, 1973.

(2)   C. A. Finch, *Polyvinyl Alcohol - Developments*, John Wiley & Sons: London, 1992.

(3)   J. G. Pritchard, *Poly(Vinyl Alcohol): Basic Properties and Uses*, Gordon and Breach: London, 1970.

(4)   C. M. Hassan, N. A. Peppas, *Adv. Polym. Sci.* **2000**, *153*, 37.

(5)   *Polymers of Biological and Biomedical Significance* (Eds.: S. W. Shalaby, Y. Ikada, R. Langer, J. Williams), ACS Symp. Ser. 540, American Chemical Society: Washington DC, 1994.

(6)   K. Tamura, O. Ike, S. Hitomi, J. Isobe, Y. Shimizu, M. Nambu, *ASAIO transactions / American Society for Artificial Internal Organs* **1986**, *32*, 605.

(7)   N. A. Peppas, N. K. Mongia, *Eur. J. Pharm. Biopharm.* **1997**, *43*, 51.

(8)   I. Galeska, T.-K. Kim, S. D. Patil, U. Bhardwaj, D. Chatttopadhyay, F. Papadimitrakopoulos, D. J. Burgess, *AAPS J.* **2005**, *7*, E231.

(9)   X. Liu, K. Nakamura, A. M. Lowman, *Soft Materials* **2003**, *1*, 393.

(10)   Q. B. Bao, G. M. McCullen, P. A. Higham, J. H. Dumbleton, H. A. Yuan, *Biomaterials* **1996**, *17*, 1157.

(11)   A. Joshi, G. Fussell, J. Thomas, A. Hsuan, A. Lowman, A. Karduna, E. Vresilovic, M. Marcolongo, *Biomaterials* **2005**, *27*, 176.

(12)   S.-H. Hyon, W.-I. Cha, Y. Ikada, M. Kita, Y. Ogura, Y. Honda, *J. Biomater. Sci. Polym. Ed.* **1994**, *5*, 397.

(13)   N. Buhler, H.-P. Haerri, M. Hofmann, C. Irrgang, A. Muhlebach, B. Muller, F. Stockinger, *Chimia* **1999**, *53*, 269.

(14)   M. Oka, K. Ushio, P. Kumar, K. Ikeuchi, S. H. Hyon, T. Nakamura, H. Fujita, *Proc. Inst. Mech. Eng. [H]* **2000**, *214*, 59.

(15)   W. Swieszkowski, D. N. Ku, H. E. N. Bersee, K. J. Kurzydlowski, *Biomaterials* **2006**, *27*, 1534.

(16)   Y. You, W. H. Park, B. M. Ko, B.-M. Min, *J. Mater. Sci.: Mater. Med.* **2004**, *15*, 297.

(17)   L. Varshney, *BARC Newsletter* **2003**, *239*, 10.

(18)   S. R. Stauffer, N. A. Peppas, *Polymer* **1992**, *33*, 3932.

(19)   A. S. Hickey, N. A. Peppas, *J. Membr. Sci.* **1995**, *107*, 229.

(20)   N. A. Peppas, J. E. Scott, *J. Controlled Release* **1992**, *18*, 95.

(21)   F. Yokoyama, I. Masada, K. Shimamura, T. Ikawa, K. Monobe, *Colloid Polym. Sci.* **1986**, *264*, 595.

(22)   P. J. Willcox, D. W. Howie, Jr., K. Schmidt-Rohr, D. A. Hoagland, S. P. Gido, S. Pudjijanto, L. W. Kleiner, S. Venkatraman, *J. Polym. Sci., Part B: Polym. Phys.* **1999**, *37*, 3438.

(23)   F. Urushizaki, H. Yamaguchi, K. Nakamura, S. Numajiri, K. Sugibayashi, Y. Morimoto, *Int. J. Pharm.* **1990**, *58*, 135.

(24)   R. Ricciardi, G. D'Errico, F. Auriemma, G. Ducouret, A. M. Tedeschi, C. De Rosa, F. Laupretre, F. Lafuma, *Macromolecules* **2005**, *38*, 6629.

(25)   R. Ricciardi, F. Auriemma, C. De Rosa, F. Laupretre, *Macromolecules* **2004**, *37*, 1921.

(26)   R. Ricciardi, F. Auriemma, C. De Rosa, *Macromol. Symp.* **2005**, *222*, 49.

(27)   C. H. Cholakis, M. V. Sefton, *Polym. Prepr.* **1983**, *24*, 64.

(28)   B. Gander, R. Gurny, E. Doelker, N. A. Peppas, *Pharm. Res.* **1989**, *6*, 578.

(29)   F. Horkay, M. Nagy, *Polym. Bull.* **1980**, *3*, 457.

(30)   S. Kurihara, S. Sakamaki, S. Mogi, T. Ogata, T. Nonaka, *Polymer* **1996**, *37*, 1123.

(31)   H. K. Purss, G. G. Qiao, D. H. Solomon, *J. Appl. Polym. Sci.* **2005**, *96*, 780.

(32)   W. E. Hennink, C. F. van Nostrum, *Adv. Drug Delivery Rev.* **2002**, *54*, 13.

(33)   J. E. Gough, C. A. Scotchford, S. Downes, *J. Biomed. Mater. Res.* **2002**, *61*, 121.

(34)   K. R. Stevens, N. J. Einerson, J. A. Burmania, W. J. Kao, *J. Biomater. Sci. Polym. Ed.* **2002**, *13*, 1353.

(35)   L. Marinucci, C. Lilli, M. Guerra, S. Belcastro, E. Becchetti, G. Stabellini, E. M. Calvi, P. Locci, *J. Biomed. Mater. Res., Part A* **2003**, *67A*, 504.

(36)   J. Ruiz, A. Mantecon, V. Cadiz, *J. Appl. Polym. Sci.* **2003**, *87*, 693.

(37)   V. Gimenez, A. Mantecon, J. C. Ronda, V. Cadiz, *J. Appl. Polym. Sci.* **1997**, *65*, 1643.

(38)   A. Mohlebach, B. Moller, C. Pharisa, M. Hofmann, B. Seiferling, D. Guerry, *J. Polym. Sci., Part A: Polym. Chem.* **1997**, *35*, 3603.

(39)   R. H. Schmedlen, K. S. Masters, J. L. West, *Biomaterials* **2002**, *23*, 4325.

(40)   N. Ishizuka, Y. Hashimoto, Y. Matsuo, K. Ijiro, *Colloids Surf., A* **2006**, *284-285*, 440.

(41)   V. Gimenez, J. A. Reina, A. Mantecon, V. Cadiz, *Polymer* **1999**, *40*, 2759.

(42)   F. Cavalieri, F. Miano, P. D'Antona, G. Paradossi, *Biomacromolecules* **2004**, *5*, 2439.

(43)   P. Martens, K. S. Anseth, *Polymer* **2000**, *41*, 7715.

(44)   P. A. Rundquist, P. Photinos, S. Jagannathan, S. A. Asher, *J. Chem. Phys.* **1989**, *91*, 4932.

(45)   S. A. Asher, P. L. Flaugh, G. Washinger, *Spectroscopy* **1986**, *1*, 26.

(46)   R. J. Carlson, S. A. Asher, *Appl. Spectrosc.* **1984**, *38*, 297.

(47)   J. M. Weissman, H. B. Sunkara, A. S. Tse, S. A. Asher, *Science (Washington, D. C.)* **1996**, *274*, 959.

(48)   C. E. Reese, C. D. Guerrero, J. M. Weissman, K. Lee, S. A. Asher, *J. Colloid Interface Sci.* **2000**, *232*, 76.

(49)   P. L. Flaugh, S. E. O'Donnell, S. A. Asher, *Appl. Spectrosc.* **1984**, *38*, 847.

(50)   P. A. Rundquist, R. Kesavamoorthy, S. Jagannathan, S. A. Asher, *J. Chem. Phys.* **1991**, *95*, 1249.

(51)   S. A. Asher, *EP Patent 168988*, **1986**.

(52)   F. Zeng, S. Wu, Z. Sun, H. Xi, R. Li, Z. Hou, *Sens. Actuators, B* **2002**, *B81*, 273.

(53)   J. H. Holtz, S. A. Asher, *Nature* **1997**, *389*, 829.

(54)   S. A. Asher, J. Holtz, L. Liu, Z. Wu, *J. Am. Chem. Soc.* **1994**, *116*, 4997.

(55)   K. Lee, S. A. Asher, *J. Am. Chem. Soc.* **2000**, *122*, 9534.

(56)   J. H. Holtz, J. S. W. Holtz, C. H. Munro, S. A. Asher, *Anal. Chem.* **1998**, *70*, 780.

(57)   G. Pan, R. Kesavamoorthy, S. A. Asher, *Phys. Rev. Lett.* **1997**, *78*, 3860.

(58)   S. A. Asher, J. H. Holtz, *US Patent 5854078*, 1998.

(59)   S. A. Asher, J. H. Holtz, *WO Patent 9841859*, 1998.

(60)   S. A. Asher, J. H. Holtz, *WO Patent 9819787*, 1998.

(61)   J. M. Jethmalani, W. T. Ford, *Chem. Mater.* **1996**, *8*, 2138.

(62)   S. H. Foulger, P. Jiang, A. C. Lattam, D. W. Smith, Jr., J. Ballato, *Langmuir* **2001**, *17*, 6023.

(63)   Y. Takeoka, M. Watanabe, *Langmuir* **2002**, *18*, 5977.

(64)   H. Nakamura, M. Ishii, *Langmuir* **2005**, *21*, 11578.

(65)   K. W. Kimble, J. P. Walker, D. N. Finegold, S. A. Asher, *Anal. Bioanal. Chem.* **2006**, *385*, 678.

(66)   M. Ben-Moshe, V. L. Alexeev, S. A. Asher, *Anal. Chem.* **2006**, *78*, 5149.

(67)   J. P. Walker, S. A. Asher, *Anal. Chem.* **2005**, *77*, 1596.

(68)   A. C. Sharma, T. Jana, R. Kesavamoorthy, L. Shi, M. A. Virji, D. N. Finegold, S. A. Asher, *J. Am. Chem. Soc.* **2004**, *126*, 2971.

(69)   V. L. Alexeev, S. Das, D. N. Finegold, S. A. Asher, *Clin. Chem. (Washington, DC, U. S.)* **2004**, *50*, 2353.

(70)   C. E. Reese, S. A. Asher, *Anal. Chem.* **2003**, *75*, 3915.

(71)   M. Kamenjicki, I. K. Lednev, A. Mikhonin, R. Kesavamoorthy, S. A. Asher, *Adv. Funct. Mater.* **2003**, *13*, 774.

(72)   S. A. Asher, A. C. Sharma, A. V. Goponenko, M. M. Ward, *Anal. Chem.* **2003**, *75*, 1676.

(73)   S. A. Asher, V. L. Alexeev, A. V. Goponenko, A. C. Sharma, I. K. Lednev, C. S. Wilcox, D. N. Finegold, *J. Am. Chem. Soc.* **2003**, *125*, 3322.

(74)   V. L. Alexeev, A. C. Sharma, A. V. Goponenko, S. Das, I. K. Lednev, C. S. Wilcox, D. N. Finegold, S. A. Asher, *Anal. Chem.* **2003**, *75*, 2316.

(75)   S. A. Asher, S. F. Peteu, C. E. Reese, M. X. Lin, D. Finegold, *Anal. Bioanal. Chem.* **2002**, *373*, 632.

(76)   C. E. Reese, M. E. Baltusavich, J. P. Keim, S. A. Asher, *Anal. Chem.* **2001**, *73*, 5038.

(77)   S. A. Asher, V. L. Alexeev, I. K. Lednev, A. C. Sharma, C. Wilcox, *US Patent 2003027240*, 2003.

(78)   S. A. Asher, C. E. Reese, *US Patent 2002164823*, 2002.

(79)   S. A. Asher, C. E. Reese, *US Patent 2002031841*, 2002.

(80)   S. A. Asher, M. Kamenjicki, I. K. Lednev, V. Meier, *WO Patent 2001063345*, 2001.

(81)   H. Saito, Y. Takeoka, M. Watanabe, *Chem. Commun.* **2003**, 2126.

(82)   M. K. Maurer, I. K. Lednev, S. A. Asher, *Adv. Funct. Mater.* **2005**, *15*, 1401.

(83)   M. Kamenjicki, R. Kesavamoorthy, S. A. Asher, *Ionics* **2004**, *10*, 233.

(84)   M. Kamenjicki, I. K. Lednev, S. A. Asher, *J. Phys. Chem. B* **2004**, *108*, 12637.

(85)   M. Kamenjicki, S. A. Asher, *Macromolecules* **2004**, *37*, 8293.

(86)   P. J. Flory, *Principles of Polymer Chemistry*, Cornell University Press: New York, 1953.

(87)   M. Annaka, T. Tanaka, *Nature* **1992**, *355*, 430.

(88)   S. Mafe, J. A. Manzanares, A. E. English, T. Tanaka, *Phys. Rev. Lett.* **1997**, *79*, 3086.

(89)   S. E. Kudaibergenov, V. B. Sigitov, *Langmuir* **1999**, *15*, 4230.

(90)   X. Xu, A. V. Goponenko, S. A. Asher, *J. Am. Chem. Soc.* **2008**, 130, 3113-3119.

(91)   J. T. Baca, D. N. Finegold, S. A. Asher, *Analyst* **2008**, *133*, 385-390.

(92)   D. Ceylan, M. M. Ozmen, O. Okay, *J. Appl. Polym. Sci.* **2006**, *99*, 319.

(93)   R. C. Allen, *US Patent 5159049*, 1992.

(94)   R. C. Allen, B. J. Radola, *US Patent 4746551*, 1988.

(95)   M. Y. Arica, G. Bayramoglu, *Biochemical Engineering Journal* **2004**, *20*, 73.

(96)   S. I. Brahim, D. Maharajh, D. Narinesingh, A. Guiseppi-Elie, *Anal. Lett.* **2002**, *35*, 797.

(97)   H. Lei, W. Wang, L.-L. Chen, X.-C. Li, B. Yi, L. Deng, *Enzyme Microb. Technol.* **2004**, *35*, 15.

3.0 POLYMERIZED CRYSTALLINE COLLOIDAL ARRAY SENSING OF HIGH GLUCOSE CONCENTRATIONS

Ward Muscatello, M. M.; Stunja, L. E.; Asher, S. A., *submitted to Analytical Chemistry,* **2008**.

We are developing photonic crystal glucose sensing materials to continuously monitor relatively high glucose concentrations, such as found in blood. We modified our synthetic fabrication methodologies in order to increase the glucose concentration range and to increase the reproducibility of our PCCA fabrication. We have also advanced our understanding of the sensing response by developing a mechanical method to independently determine the hydrogel crosslink density. Our investigation of the sensing mechanism indicates that glucose binding depends mainly on the boronic acid concentrations and affinities, and we have determined the binding constant of 2-fluoro-5-aminophenyl boronic acid for glucose under physiological conditions. We have examined the dependence of glucose sensing upon interferences by other species that ligand to boronic acids, such as lactate and human serum albumin. We examined the stability of our sensors over a period of weeks at room temperature and demonstrated that we could further stabilize our sensing materials by reversibly dehydrating it for storage.

3.1 INTRODUCTION

Hyperglycemia has been shown to be associated with an increased mortality, morbidity, and length of hospital stay for patients suffering from a range of surgical and trauma diagnoses, including acute neurologic disease, cardiac surgery, and stroke[1-11]. In America, diabetes afflicts 23.6 million people (8.0% of the population)[12]. People with diabetes have increased hospitalization, with an increased length of stay and a resulting increase in overall care costs[13-16].

In addition to the need for glucose monitoring in the case of patients with chronic diabetes mellitus, there is a critical need for monitoring glucose levels in non-diabetic acute care patients, since large variations in blood glucose concentration have been observed in non-diabetic patients as a common consequence of surgery or acute illness[9,17,18]. The American Diabetes Association recommends tight control of blood glucose levels for hospitalized critically ill patients[19]. In several recent studies, it has been shown that tight control of blood glucose levels has a significant positive effect on the health of patients in surgical and medical intensive care units, particularly for those suffering from stress-induced hyperglycemia[20-22]. This positive outcome results in substantial cost of care savings[23].

Establishing a means of reliable, relatively noninvasive, and continuous glucose monitoring would result in markedly improved outcomes for inpatients with diagnosed diabetes mellitus and for those patients who experience acute care induced hyperglycemia[1,21,22,24]. The crucial demand for continuous, accurate, and relatively noninvasive glucose sensing methods has motivated the development of a wide array of sensing materials and methodologies. Many of these approaches to glucose monitoring have utilized boronic acid derivatives to bind glucose[25-42]. For example, boronic acid derivatives have been utilized in the development of fluorescence, colorimetric and electrochemical based glucose sensing technologies[31,36,38].

45
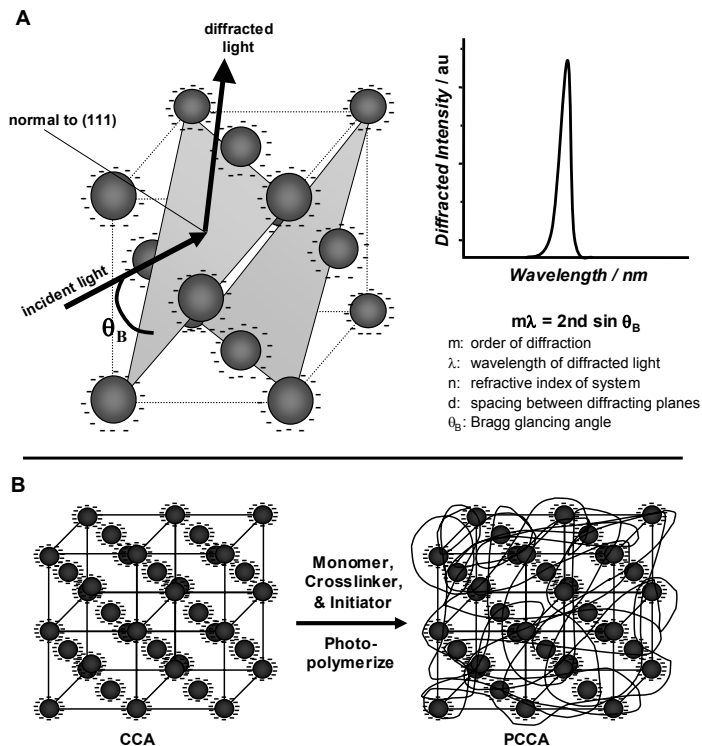
Figure 3-1. (A) Crystalline Colloidal Arrays (CCA) assemble due to the electrostatic repulsion between the highly-charged, monodisperse polystyrene particles. The spacing between particles is such that they diffract visible light according to Bragg's law. (B) Polymerized Crystalline Colloidal Arrays (PCCA) are formed by polymerizing a hydrogel network around the CCA.

We recently reported on the development of a boronic acid based glucose sensor[43-47], which utilizes our previously developed polymerized crystalline colloidal array sensing technology[48-54]. Our photonic crystal hydrogel consists of a mesoscopically periodic array of colloidal particles that self-assembles into a highly-ordered crystalline colloidal array (CCA), with a lattice spacing that Bragg diffracts visible light (Figure 3-1A)[55-62]. When the CCA is polymerized within a hydrogel (PCCA), the PCCA optically reports on volume changes experienced by the hydrogel, since the observed diffraction wavelength is directly related to the

spacing between lattice planes (Figure 3-1B). We applied this motif to chemical sensing by functionalizing the hydrogel such that changes in the concentration of the analyte of interest actuates changes in the hydrogel volume and, thereby, the diffraction wavelength. We developed intelligent PCCA (IPCCA) for use in the detection of analytes, including glucose[43-47], cations[63-66], ammonia[67], creatinine[68], pH[69,70], and organophosphates[71,72].
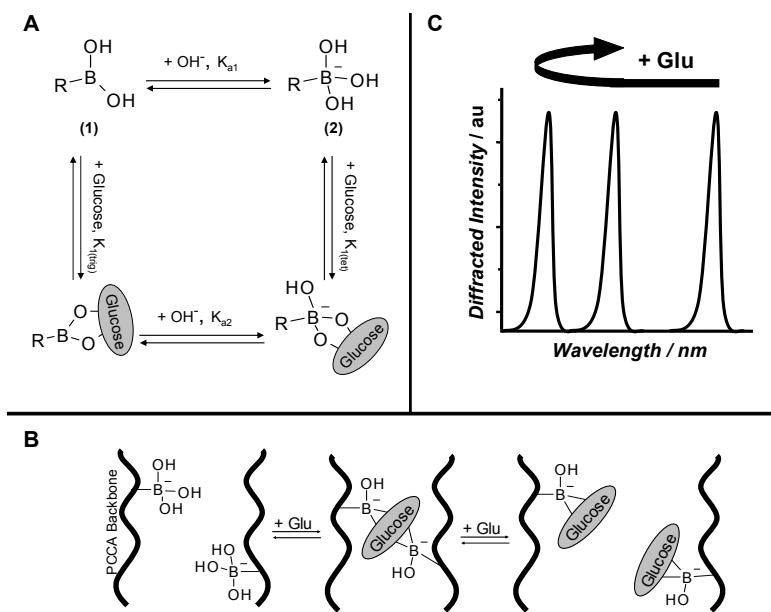
Figure 3-2. (A) pH-dependent equilibria involved in the 1:1 interaction between boronic acid and glucose. Boronic acid can bind glucose both in its neutral trigonal form (1) and its charged tetrahedral form (2). (B) Boronic acid recognition molecules are tethered to the PCCA hydrogel backbone. Upon binding glucose, additional crosslinks are formed within the hydrogel, as 2:1 boronate-glucose complexes form. At higher glucose concentrations, these additional crosslinks are broken as 1:1 boronate-glucose complexes form. (C) Illustration of how the diffraction from the PCCA reports on the volume changes experienced by the hydrogel. As the hydrogel shrinks due to additional crosslink formation, the diffraction blue-shifts. The bisboronate-glucose crosslinks are broken at higher concentrations of glucose. Thus, the hydrogel swells and the diffraction then red-shifts.

47

For sensing glucose, boronic acid recognition molecules are tethered to the PCCA hydrogel backbone. Upon binding glucose, additional bisboronate-glucose crosslinks are formed within this originally lightly crosslinked hydrogel, shrinking the hydrogel volume and blue-shifting the diffraction wavelength in proportion to the concentration of glucose bound (Figure 3-2)[44]. Much of our previous work focused on the development of a glucose-sensing material that functions under physiological pH and ionic strength conditions for the detection of the very low concentrations of glucose, as found in tear fluid (~0.1 mM)[43,73]. In the work here, we further developed our sensing material for monitoring higher glucose concentrations, such as found in blood (~5 mM)[74].

3.2   EXPERIMENTAL SECTION

3.2.1   Materials

2,2-diethoxyacetophenone (98%, DEAP) was purchased from Acros Organics. Phosphate Buffered Saline (0.1 M phosphate, 0.15 M NaCl, pH 7.2, PBS), MES Buffered Saline [0.1 M 2-(morpholino)ethanesulfonic acid, 0.9% NaCl, pH 4.7, MES], and 1-ethyl-3-(3-dimethylaminopropyl) carbodiimide hydrochloride (EDC) were purchased from Pierce Biotechnology. Acrylamide (98%, AA), N,N'-methylenebisacrylamide (98%, BisAA), N,N,N',N'-tetramethylethylenediamine (98%, TEMED), sodium L-lactate (99%), D(+)-glucose (99.5%), and Alizarin Red S (ARS) were purchased from Sigma-Aldrich. HCl, NaOH, and NaCl were purchased from J.T. Baker. Dimethyl sulfoxide (DMSO) was purchased from Thermo Fisher Scientific, Inc. 5-amino-2-fluorophenylboronic acid (98%, BA) was purchased from

Asymchem. Gel support films were purchased from Bio-Rad Laboratories. All chemicals were used as received. Deionized water (Barnstead Nanopure Water Purification System) was used for solution preparation.

3.2.2 CCA Preparation

Monodisperse, highly-charged polystyrene colloids were prepared via a modified emulsion polymerization as reported elsewhere[57], with additional initiator and charged monomer being added near the end of the polymerization process to increase the surface charge on the particles. We used ~16% w/w suspensions of 145 nm diameter CCA dispersed in pure water. The colloidal particles were cleaned via dialysis against deionized water and subsequently shaken with ion-exchange resin.

3.2.3 PCCA Hydrogel Preparation

The PCCA was synthesized by free radical polymerization in the absence of oxygen. In a typical recipe, 0.1 g AA, 0.002 g BisAA, ion-exchange resin, and 2.0 g CCA were vortexed together in a small glass vial. The vial was wrapped in Al foil and 20 μL of DEAP (20 % in DMSO) was added. The solution was vortexed again. The polymerization solution and polymerization cell, which consisted of two quartz plates separated by a 125 μm parafilm spacer with a gel support film containing surface vinyl groups used as one face of the cell, were degassed in a vacuum dissector and then filled with nitrogen in a glove bag.

Within the glove bag, the polymerization solution was centrifuged, injected into the cell, and then sealed within a Ziploc bag, so as to exclude oxygen during polymerization. The system

was photopolymerized with UV light from two Blak Ray (365 nm) mercury lamps. The resulting PCCA, which was covalently affixed to the gel support film during polymerization, was rinsed with large quantities of pure water.

For the determination of permanent effective crosslink density, the PCCA were prepared using a 250 µm parafilm spacer and without the gel support film.

3.2.4 PCCA Functionalization

Amides on the PCCA hydrogel backbone were converted to carboxylates via hydrolysis in a 0.1 M NaOH and 10% v/v TEMED solution for 1.5 hours, unless otherwise noted. The hydrolyzed PCCA was washed extensively with 150 mM NaCl solution. A NaCl solution was used to avoid stress on the immobilized hydrogel due to hydrogel swelling which would occur in pure water due to the Donnan potential resulting from the immobilized carboxylate groups on the hydrogel backbone.

In order to attach BA recognition groups to the hydrogel backbone, the PCCA was immersed in a MES buffer solution containing 25 mM BA and 25 mM EDC (pH 4.7) for 1 hr. Additional EDC was then added to the initial coupling solution, to bring the total concentration of EDC to 50 mM, so as to ensure complete coupling between the hydrogel carboxyl groups and the BA amino groups. The IPCCA were extensively washed with a PBS buffer solution (pH 7.4).

3.2.5   PCCA Permanent Effective Crosslink Determination

Oscillatory shear measurements were performed with an AR2000 Rheometer (TA Instruments) using a 25 mm parallel plate geometry, with the temperature being maintained at 25 $^{\circ}$C by a Peltier stage. After loading the sample, water was added around the edge of the sample to prevent evaporation of the water in the hydrogel during the experiment. The storage modulus was measured using a frequency-sweep between 0.1 to 100 rad/s at a fixed oscillatory shear strain of 5%. As the material was analyzed at low strains, no further modification of the stage was necessary to prevent slip of the material.

3.2.6   BA Binding Constant Determination

The binding constant of BA to glucose was determined using an ARS competitive binding assay method[42,75,76]. The binding constant of BA to ARS was first determined by titrating an ARS solution ($9x10^{-6}$ M ARS) with a BA solution ($2x10^{-3}$ M BA, $9x10^{-6}$ M ARS) and monitoring the absorbance changes upon complex formation. The BA-ARS complex solution ($2x10^{-3}$ M BA, $9x10^{-6}$ M ARS) was then titrated with a BA-ARS-glucose solution ($2x10^{-3}$ M BA, $9x10^{-6}$ M ARS, 1.2 M glucose) to determine the binding constant of BA to glucose. All studies were carried out in PBS at pH 7.4. The reported values are the average of duplicate titrations.

3.2.7 Diffraction Measurements

Diffraction measurements were conducted at a fixed 90° glancing angle utilizing an Ocean Optics USB2000-UV-VIS Spectrometer, a LS-1 Tungsten Halogen Light Source, and an R-series Fiber Optic Reflection Probe. Experiments were conducted in a covered petri dish, so as to avoid evaporation. Holes were drilled in the lid and secured with parafilm, allowing access for the reflection probe and addition/removal of solutions.

To characterize the response of the IPCCA to changes in glucose concentration, the hydrogel was first equilibrated in PBS buffer (pH 7.4), unless otherwise noted. Glucose was added to the testing solution by removing a small amount of buffer from the petri dish, dissolving the glucose within that buffer, and then returning this solution to the petri dish. After addition of glucose, the diffraction was monitored until it stabilized (stable diffraction value exhibited for ~30 min.). The IPCCA was rinsed between sensing runs with copious amounts of PBS buffer. The diffraction response shown is the average response at each glucose concentration for three separate pieces of a single fabricated IPCCA sensor, unless otherwise noted.

To ensure that a lack of a mutarotation equilibrium of the freshly prepared glucose solutions did not bias the diffraction response of the sensor[45], we compared the response to the solution prepared as discussed above to that which occurred upon addition of a pre-equilibrated concentrated glucose solution, prepared in PBS buffer (pH 7.4) several hours prior to the addition. Although the kinetics of the response differed, the final spectral response was essentially identical. Thus, all sensing runs reported here were accomplished by the dissolution of the solid within the equilibration buffer at the time of testing.

3.3   RESULTS AND DISCUSSION

3.3.1   Sensing Response Dependence on Boronic Acid Concentration

We investigated the dependence of the glucose sensing response on the concentration of BA incorporated in the IPCCA. We previously found that sensors with low concentrations of incorporated boronic acid recognition groups utilized a supramolecular bisbidentate glucose-boronate complex, where Na^+ chelating agents [polyethylene glycol (PEG) or crown ethers] were required for crosslink formation[43,44]. We subsequently found that glucose-boronate bisbidentate crosslinks occurred in the absence of such chelating agents for high concentrations of boronic acid[45].

In our new studies reported here, we surprisingly find that Na^+ chelating agents are unnecessary for a response to glucose in high ionic strength solutions, even for low concentrations of incorporated BA groups. As seen in Figure 3-3A, sensors with both relatively low and high BA concentrations exhibit a blue-shift in the diffracted wavelength upon glucose binding in the absence of PEG or crown ethers. IPCCA with different concentrations of BA were prepared by hydrolyzing the material for different times (0.5 hour and 1.5 hour) prior to coupling with BA. As the boronic acid is tethered to the hydrogel through the carboxyl groups produced during hydrolysis, this resulted in sensors with different concentrations of incorporated BA.

We characterized the response of these materials by plotting the linear deformation factor, $\alpha = \lambda/\lambda^*$, where λ and λ^* are the diffracting wavelengths at the glucose concentration of interest and in the absence of glucose, respectively. The observed diffraction wavelength decrease is due to the additional crosslinks formed within the hydrogel as the tethered boronic

acid moieties bind glucose in 2:1 complexes. The increase in the effective crosslink concentration shrinks the hydrogel volume, blue-shifting the diffraction.

The most likely explanation of our earlier erroneous conclusions is that the sensors previously prepared in the absence of chelators all contained an insufficient concentration of boronic acid, which biased our results. In fact, our earlier studies did show occasional unexplained, but rare, failures to couple boronic acid derivatives to the hydrogel.
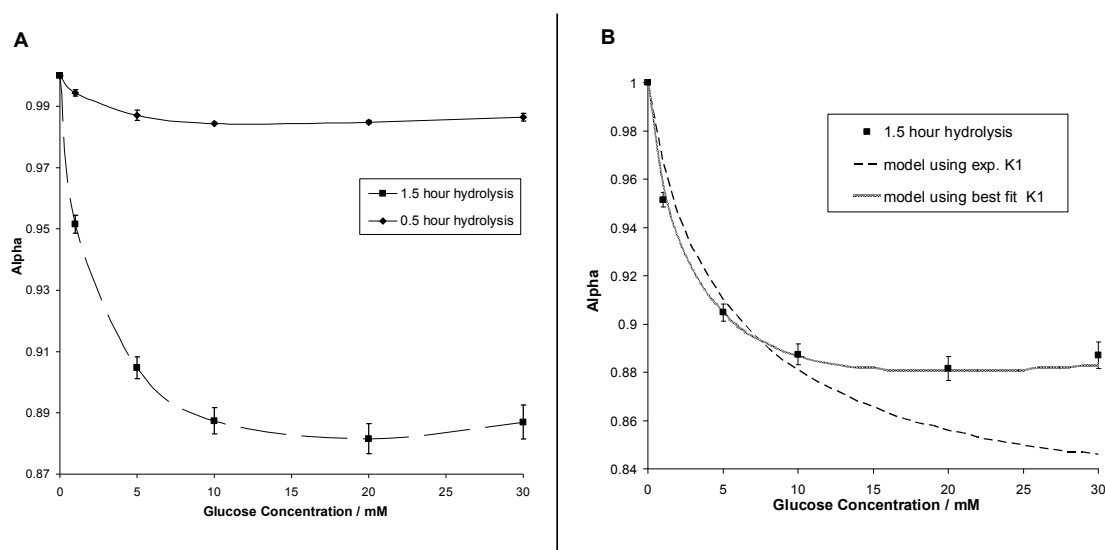
Figure 3-3. (A) The magnitude of the diffraction shift depends on the concentration of boronic acid (BA) attached to the hydrogel backbone. The mechanism of the response is the same, both at low (0.5 hr hydrolysis) and higher (1.5 hr hydrolysis) BA concentrations. The additional crosslinks formed within the hydrogel as the tethered BA groups bind glucose in 2:1 complexes shrinks the hydrogel volume, blue-shifting the diffraction. (Lines added to aid the eye.) (B) Using experimentally determined value of association constant of BA for glucose (dashed line), our model somewhat fits the experimental data for lower glucose concentrations, but fails at higher glucose concentrations. We, however, find that we can well fit the experimental data if we use larger association constants (solid line), which indicates that the effective association constants of the bound complexes are affected by the attached hydrogel and that solution equilibria are too simplistic to successfully model the interactions within the hydrogel matrix.

54

3.3.2 Revised Modeling of IPCCA Sensing Response

The sensing mechanism employed in our IPCCA material, which employs bisbidentate complex formation, can be modeled[44] by utilizing Flory's model[77] for the swelling of polymer network structures by requiring that the total osmotic pressure at equilibrium equal zero:

$$\Pi_T = \Pi_M + \Pi_E + \Pi_{Ion} = 0.$$

Equation 3-1

Π_M is the osmotic pressure arising from the change in free energy of mixing:

$$\Pi_M = -\frac{\partial \Delta G_M}{\partial V} = -\frac{RT}{V_s}\left[\ln\left(1-\frac{V_0}{V}\right)+\frac{V_0}{V}+\chi\left(\frac{V_0}{V}\right)^2\right],$$

Equation 3-2

Π_E is the osmotic pressure arising from the change in the elastic free energy:

$$\Pi_E = -\frac{\partial \Delta G_E}{\partial V} = -RT\cdot\upsilon_e\left[\left(\frac{V_m}{V}\right)^{1/3}-\frac{1}{2}\frac{V_m}{V}\right]-RT\cdot c_{B2G}$$

Equation 3-3

and Π_{Ion} is the osmotic pressure due to the Donnan potential, arising from the difference in mobile ion concentration inside and outside of the hydrogel:

$$\Pi_{Ion} = RT(c_+ + c_- - c_+^* - c_-^*)$$

Equation 3-4

where R is the universal gas constant, T is the temperature, χ is the Flory-Huggins interaction parameter, V_s is the molar volume of the solvent, υ_e is the effective crosslink density of the hydrogel network, c_{B2G} is the concentration of the additional crosslinks formed upon glucose binding, V is the current volume of the hydrogel, V_m is the volume of the relaxed hydrogel

network, V_0 is the volume of the dry hydrogel network, c_+ and c_- are the concentrations of mobile cations and anions inside the hydrogel, and c_+^* and c_-^* are the concentrations of mobile cations and anions outside the hydrogel.

As the Donnan potential is negligible in high ionic strength solutions and should insignificantly affect the hydrogel volume, the total osmotic pressure thereby results from changes in the free energies of mixing and elasticity. At equilibrium, $\Pi_M + \Pi_E = 0$. In addition, we ignore changes in the value of χ upon glucose binding, and we assume that the volume changes experienced by the hydrogel derive primarily from changes in the effective number of crosslinks, which are formed and broken upon changes in the glucose concentration.

The equilibria involved in glucose binding by boronic acid are complex, as glucose can be bound by both the neutral trigonal and anionic tetrahedral forms of boronic acid. For simplicity's sake, at constant pH, we assume two equilibria and two effective binding constants to denote the overall binding of glucose by boronic acid compounds (in both trigonal and tetrahedral forms) in 1:1 and 2:1 complexes:

$$B + G \overset{K_1}{\Longleftrightarrow} BG \qquad \qquad K_1 = \frac{[BG]}{[B][G]}$$

Equation 3-5

$$2B + G \overset{K_2}{\Longleftrightarrow} B_2G \qquad \qquad K_2 = \frac{[B_2G]}{[B]^2[G]} \; .$$

Equation 3-6

Using the total concentration of boronic acid sites within the IPCCA

$$C_T = [B] + [BG] + 2[B_2G] = [B] + K_1[B][G] + 2K_2[B]^2[G]$$

Equation 3-7

we determine the concentration of glucose-boronate crosslinks within the IPCCA, [B$_2$G],

$$c_{B2G} = [B_2G] = K_2[B]^2[G]$$

Equation 3-8

at any given glucose concentration, [G].

The volume changes experienced by the IPCCA upon glucose binding are modeled by calculating the concentration of 2:1 boronate:glucose complexes formed as a function of the glucose concentration and making use of the relationship between hydrogel volume and diffraction wavelength:

$$\left(\frac{V}{V^*}\right)^{\frac{1}{3}} = \frac{\lambda}{\lambda^*},$$

Equation 3-9

where V and V^* are the hydrogel volumes at the glucose concentration of interest and in the absence of glucose, respectively.

We are now able to constrain our model because we directly measured the effective crosslink density of the hydrogel in the absence of glucose. We found an effective permanent crosslink concentration of 0.8 mM, which is ~2-fold smaller than the 1.46 mM previously estimated from less reliable elastic deformation measurements[70].

We experimentally determined the permanent effective crosslink density by using mechanical measurements to determine the shear storage modulus (G′). The effective crosslink density, υ_e, can be determined from the experimentally determined shear storage modulus and the polymer volume fraction (ϑ)[77, 78]:

$$G' = \upsilon_e RT \vartheta^{\frac{1}{3}}.$$

Equation 3-10

57

We estimated the Flory-Huggins interaction parameter, $\chi = 0.513$, from hydrogel swelling in the absence of glucose. The concentration of BA within the hydrogel was determined by boron elemental analysis (Columbia Analytical Services, Tucson, AZ).

We determined the association constant of 5-amino-2-fluoro-phenylboronic acid and glucose by using an ARS competitive assay[42,75,76,79]. The effective binding constant of BA to glucose in PBS at pH 7.4 was found to be $K_1 = 16\,\mathrm{M}^{-1}$, which is much lower than the binding constant of 370 M^{-1} we used to model the response of our previous generation of photonic crystal glucose sensors that utilized 4-amino-3-fluorophenylboronic acid[43,44]. However, this $K_1 = 16\,\mathrm{M}^{-1}$ value is close to those of other phenylboronic acid derivatives recently determined.[42,76]

We attempted to model of our sensing response using this $K_1 = 16\,\mathrm{M}^{-1}$ association constant for 1:1 boronate-glucose complex formation and a slightly smaller value of $K_2 = 12\,\mathrm{M}^{-2}$ for 2:1 boronate-glucose complex formation. We utilized a lower K_2 value to account for the expected decreased binding constant to the second glucose cis diol groups and to account for an effective decrease in the availability of the second boronic acid derivative due to the constraints imposed by the hydrogel. Figure 3-3B illustrates our best modeling of the IPCCA diffraction response for glucose, for an incorporated BA concentration of 170 mM and these K_1 and K_2 values. Our model somewhat fits the experimental data for lower glucose concentrations, but fails at higher glucose concentrations. We, however, find that we can well fit the experimental data if we use a $K_1 = 50\,\mathrm{M}^{-1}$ and $K_2 = 18\,\mathrm{M}^{-2}$, which indicates that the effective association constants of the bound complexes are affected by the attached hydrogel. It is no surprise that K_2 would be decreased compared to K_1, as discussed above. The increase in

K_1 is more difficult to explain; it could result from a stabilization of the complex by the hydrogel environment.
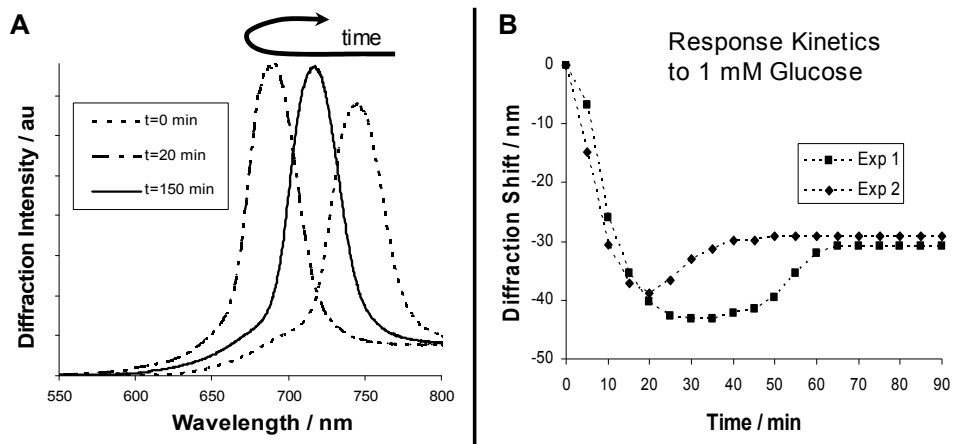
Figure 3-4. Dependence of IPCCA response on time. (A) The diffraction of the IPCCA is shown at 0 min, 20 min, and 150 min after addition of 1 mM glucose. Initially, the sensor diffraction blue-shifts in response to the addition of 1 mM glucose. Later, the diffraction begins to slowly red-shift before finally stabilizing. The prompt large blue-shift followed by a slow red-shift likely results from polymer relaxation. Initially the hydrogel volume is dominated by glucose-bisboronate linkages involving nearest neighbor crosslinks formed initially at the moment of glucose exposure. At a longer time scale the glucose binding equilibrates within the system, such that the equilibrium crosslinks store the minimum elastic energy, which results in an increased equilibrium gel volume near the surface compared to that initially formed, which red-shifts the diffraction. (B) When a sensor is put through a second sensing run (after rinsing in buffer), the initial blue-shift is smaller and equilibrium is reached in a shorter time frame. Lines are added to aid the eye.

Our previous modeling required higher values of K_2 to model the large diffraction blue-shifts observed at that time for low glucose concentrations. We now find that the measurement timeframe was insufficient; our sensors had not reached equilibrium. We find that the hydrogel

59

diffraction does not plateau at the point of the furthest blue-shift; rather, the hydrogel then slowly red-shifts back before finally plateauing (Figure 3-4A).

This prompt large blue-shift followed by a slow red-shift most likely results from hydrogel polymer relaxation. This is confirmed by the fact that the kinetics are sped up by exercising the hydrogel (Figure 3-4B).

Initially the hydrogel volume is dominated by glucose-bisboronate linkages involving instantaneous nearest neighbor crosslinks formed at the point of glucose binding. At longer times the glucose binding hydrogel complexation equilibrates such that the equilibrium crosslinked network stores the minimum elastic energy. Since the observed diffraction monitors the lattice spacing within the first ~50 layers of the embedded CCA, we are monitoring the hydrogel polymer relaxation within the outermost layer of the sensor. This relaxation process is obviously slower than the initial formation of glucose crosslinks.

3.3.3 Sensing Response Dependence on L-Lactate

Our glucose sensor must be free from significant interferences from the non-glucose constituents of blood. Lactate, a known constituent of blood, is known to bind to boronic acid derivatives[80-82]. We measured the impact of a range of lactate concentrations (2 mM to 45 mM) on our IPCCA glucose sensing response (Figure 3-5). These results clearly show that competitive binding of lactate to boronic acids within our IPCCA reduces the bisbidentate glucose crosslink concentrations. The decrease in response to glucose, and deviation from saturation at high glucose concentrations, becomes more pronounced at higher lactate concentrations.
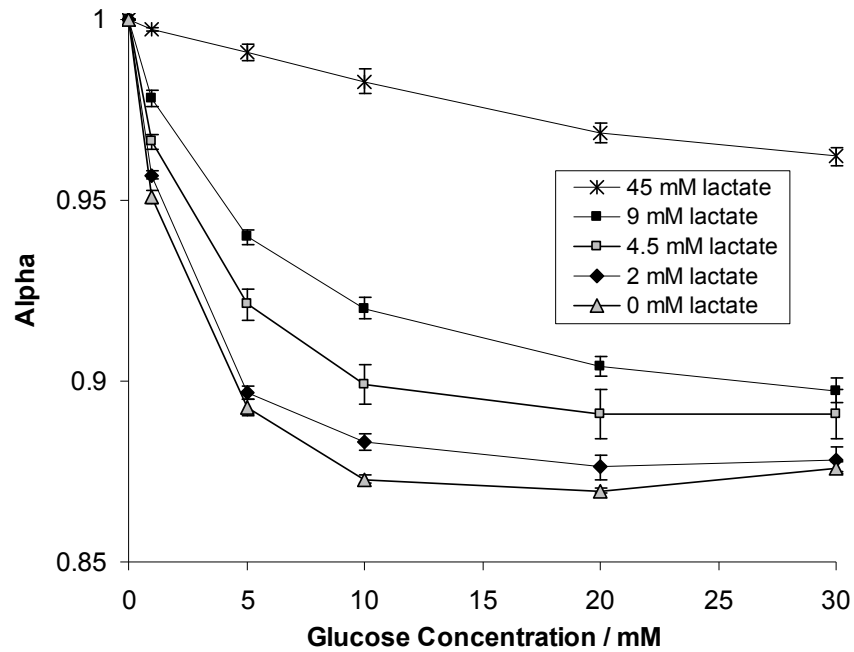
Figure 3-5. IPCCA glucose response dependence on L-lactate concentration. The average experimentally determined diffraction response of a glucose-sensitive IPCCA at varying concentrations of glucose and lactate. The alteration in the IPCCA sensing response to glucose, due to the competitive binding of the boronic acid to lactate, becomes more pronounced at higher lactate concentrations. (Lines are added to aid the eye. The 0 mM lactate data points are the average of 4 sensing runs where the sensors were taken from two separate pieces of an IPCCA fabricated in the same fashion as the IPCCA used for the sensing runs in the presence of lactate.)

This competitive binding contribution can be modeled by adding the additional equilibrium that involves boronate-lactate binding:

$$B + L \overset{K_3}{\Leftrightarrow} BL \qquad\qquad \mathrm{K}_3 = \frac{[\mathrm{BL}]}{[\mathrm{B}][\mathrm{L}]}$$

Equation 3-11

61

Now the total concentration of boronic acid sites within the IPCCA is:

$$C_T = [B] + [BG] + 2[B_2G] + [BL] = [B] + K_1[B][G] + 2K_2[B]^2[G] + K_3[B][L],$$

Equation 3-12

such that the concentration of additional crosslinks formed will be decreased by the formation of lactate-boronate complexes.

Since the lactate concentration in a resting adult lies between 0.36-0.75 mM[74], our Figure 3-5 data indicate that lactate will insignificantly impact IPCCA monitoring of glucose in blood, as there was only a 0.5% decrease in alpha for 5 mM glucose in the presence of 2 mM lactate. In addition, our IPCCA could utilize boronic acid derivatives that selectively bind glucose over lactate, such as the 2-acrylamidophenylboronate (2APB) derivative synthesized by Lowe et al[83]. They utilized a phenylboronate derivative stabilized in the tetrahedral form through interaction with a neighboring ortho group. Since boronic acids preferentially bind glucose in the tetrahedral form and lactate in the trigonal form, interference from lactate is reduced[81,84,85]. The stabilization of this boronic acid derivative in the tetrahedral form has the added benefit of alleviating any pH dependence of glucose binding.

Interestingly, the shrinkage of the sensor in response to glucose does not saturate at the higher lactate concentrations. This indicates that a competitive binding based sensing mechanism could be used to fabricate an IPCCA capable of monotonically responding to glucose over a large concentration range. By attaching a competitor species within the hydrogel material, and optimizing its concentration and binding constant, a near linear response of the sensor to glucose concentrations could be achieved.

3.3.4 Sensing Response Dependence on Human Serum Albumin

Human serum albumin (HSA), the most abundant protein in human serum,[74] is known to undergo glycosylation upon exposure to glucose via reaction between the sugar aldehyde group and the free amino groups of the protein[86-88]. We characterized the dependence of our IPCCA glucose response on the presence of HSA at the concentration typically found in serum (44 g/L)[74]. Figure 3-6 shows that HSA addition to the PBS solution increases the sensitivity at higher glucose concentrations, increasing the IPCCA response spectral window. The diffraction response, surprisingly, does not plateau at the higher glucose concentrations as it does in the absence of HSA.
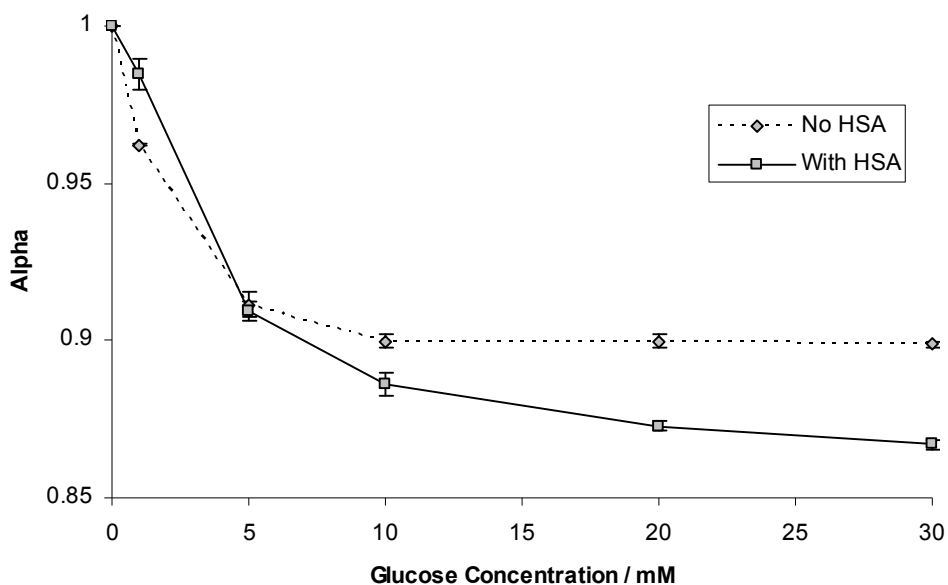
Figure 3-6. IPCCA response dependence on human serum albumin (HSA). At concentrations of HSA comparable to the average HSA concentration in serum, the overall sensitivity is increased due to changes in the free energy of mixing of the system, while the lack of a plateau in response to the range of glucose concentrations tested is due to competitive binding between the boronate and glycosylated protein in solution. (Lines are added to aid the eye).

The decreased response to addition of 1 mM glucose presumably results from "consumption" of the glucose by HSA glycosylation[89-91]. This lowers the concentration of free glucose in solution.

The overall increase in the spectral window is related to changes in the free energy of the IPCCA upon HSA binding. The boronic acid moieties on the hydrogel are capable of binding HSA, even in its nonglycosylated state[92-94]. When the IPCCA is transferred from PBS to a PBS solution containing HSA, the wavelength of diffraction red-shifts. The complexing of the tethered boronic acid to the soluble protein increases the free energy of mixing induced osmotic pressure, swelling the hydrogel. Using the diffraction values for the hydrogel swelling in the absence of glucose, we estimate a value of $\chi = 0.505$ for the system containing HSA. We modeled the response of our sensor using this new χ value, which predicts an increased glucose response consistent with that experimentally observed. The osmotic compressibility of hydrogel networks is known to depend strongly on χ, where decreases in χ result in increased compressibility[78].

The non-plateau in diffraction response can be attributed to competitive binding. As the albumin is a relatively large molecule compared to glucose, the initial association within the hydrogel hinders the accessibility of boronic acid sites that would normally be accessible to glucose. The addition of glucose, and subsequent glycosylation of the protein, elevates its role as a competitive binder. This is similar to the competitive binding phenomenon observed for lactate, as described above.

It is clear from Figure 3-6 that the presence of HSA changes the diffraction response of the IPCCA to free glucose. As the concentration of glycosylated protein in circulation can vary,

especially for those experiencing hyperglycemia[89-91], these proteins should be excluded from the sensor by a dialysis membrane for practical *in vivo* sensing.

3.3.5   Sensing Response Dependence on Ionic Strength

We examined the ionic strength dependence of the PCCA glucose sensor response in PBS solutions at total ionic strengths (TIS) of 60 mM, 300 mM and 450 mM. Figure 3-7A shows that decreasing the TIS below that of a PBS solution typically used in biological studies (450 mM) results in a decreased diffraction blue-shift.

The decreased blue-shift at low TIS results from the competition between the hydrogel shrinking, due to the additional crosslink formation, competing with the hydrogel swelling, due to the formation of the Donnan potential caused by the immobilization of a relatively high concentration of boronate anions on the hydrogel backbone, as boronic acid predominantly binds glucose in its anionic boronate form.

The Donnan potential arises from the concentration difference between the mobile counterions inside and outside of the hydrogel. When, as in this case, there is a high concentration of immobilized charged groups and their counterions within the hydrogel, the Donnan-induced osmotic pressure can be large even at relatively high ionic strengths. IPCCA response dependence on the ionic strength can be taken into account by including the Donnan potential osmotic pressure within our model[69,70]:

$$\Pi_{\text{Ion}} = RT[iC_{BA} - 2(C_s^* - C_s)]$$

Equation 3-13

65

where i is the degree of boronic acid ionization times its charge, C_{BA} is the concentration of boronic acid groups within the IPCCA, C_S^* is the concentration of mobile ions within the IPCCA and C_S is the concentration of mobile ions in the bulk solution. We will include the dependence on this Donnan potential in future modeling of this system.
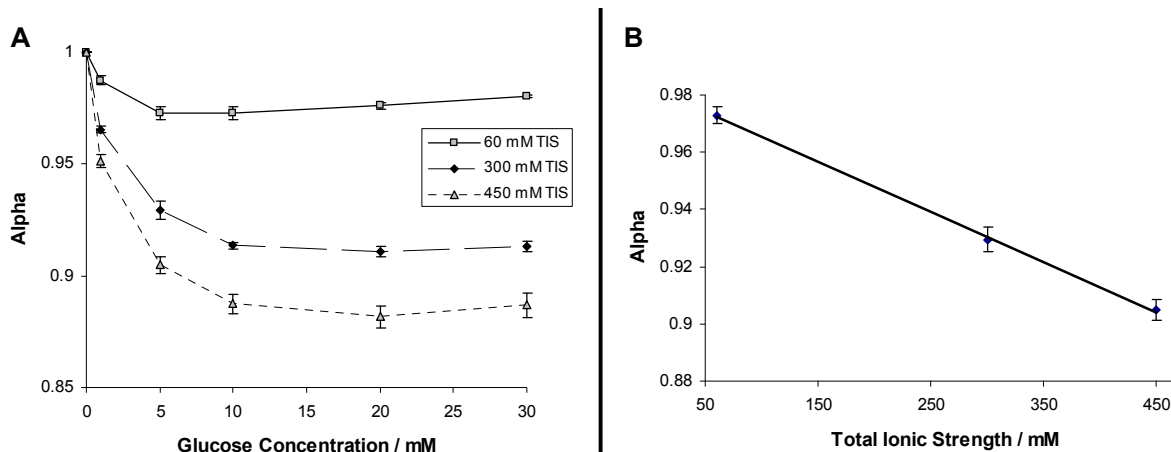
Figure 3-7. Dependence of IPCCA response on total ionic strength at pH 7.4. (A) At low ionic strength, the swelling due to the Donnan potential is large, thereby resulting in a decrease in the overall shrinking and blue-shifting of the hydrogel in response to the increase in crosslink density upon glucose binding. (Lines added to aid the eye.) (B) The observed response to glucose is linearly dependent on the total ionic strength of the solution, as can be seen by the response to 5 mM glucose at various ionic strengths.

The major electrolytes found in extracellular fluids are Na^+ and Cl^-, which together comprise the greatest fraction of osmotically active constituents of plasma. The reference intervals for Na^+ and Cl^- are 136 to 145 mM and 98 to 107 mM, respectively[74]. Taking only these intervals into consideration, one can expect a ± 4% variation in the total ionic strength of plasma. As the dependence of alpha on TIS is linear over the concentrations studied, as shown in Figure 3-7B, such a variation is TIS would translate to only a ± 0.1% variation in alpha. In acute situations, such as hyponatraemia, this variation could become more significant and could

potentially bias the sensor response. The simple incorporation of a total ionic strength IPCCA sensor[70], in tandem with the glucose sensor, would allow compensation for variations of blood ionic strength.

3.3.6   Reproducibility of Sensing Response

A successful blood glucose sensor must sense reproducibly over extended times. To investigate the reversibility and reproducibility of our PCCA sensor materials, we cycled the same IPCCA through three sensing cycles over the course of one week, monitoring different regions. We serially characterized the response for 1 mM, 5 mM and 10 mM glucose, and then thoroughly washed the sensor with PBS. Figure 3-8 shows that the sensor response is fully reversible, with the greatest variation in the average diffraction wavelength response of ±1 nm for 1 mM glucose. This measured variation is three times less than the ±3 nm variation in average diffraction wavelength response observed for three separate uncycled pieces of an IPCCA exposed to 1 mM glucose. Although the absolute diffraction wavelength across one handmade IPCCA can vary by ±15 nm, the linear deformation factor (or normalized diffraction shift) is nearly identical over the three sensing runs, indicating a fully reversible hydrogel sensing material.

3.3.7   Practical Storage for IPCCA Sensing Material

Successful sensor commercialization requires a significant sensor shelf life. A major factor in sensor lifetime is the stability of the incorporated molecular recognition molecules. Although our IPCCA demonstrates sensing stability over ~1 week when tested directly after

fabrication (Figure 3-8), longer sensor lifetimes are necessary to accommodate transportation and long-term storage. Figure 3-9 shows that the response of an IPCCA to 20 mM glucose decreases by 23% after a total of ~1 month of storage in a PBS solution at room temperature. Although we have not yet diagnosed the response degradation; we speculate that it is due to a limited lifetime of the boronic acid recognition agent when stored in an aqueous environment. Therefore, we expect that storage of this material in the dry state would result in an extended shelf-life.
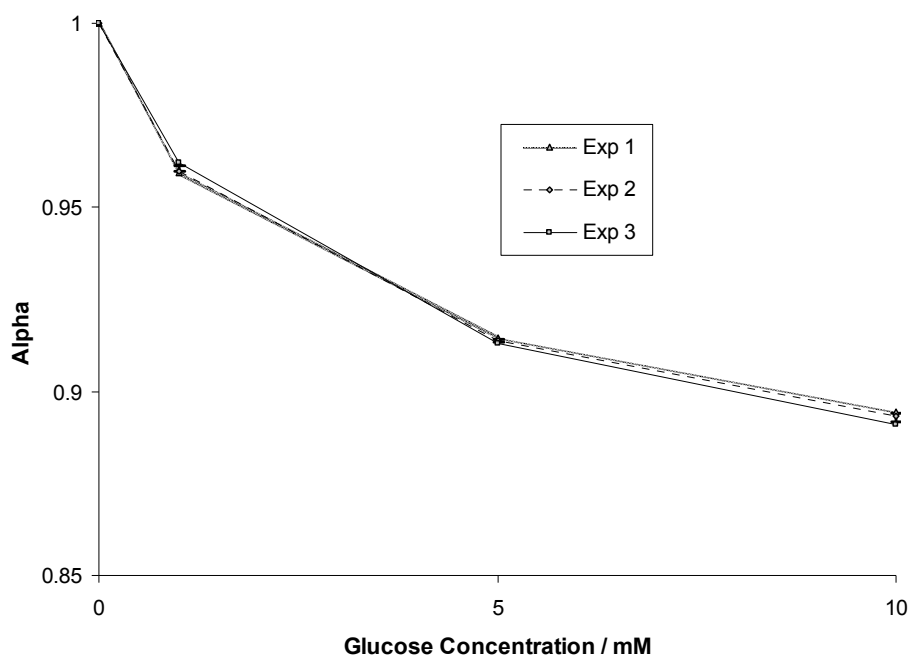
Figure 3-8. IPCCA response dependence on cycling. The same piece of IPCCA was cycled through three glucose-sensing runs over the course of one week. The sensor response was characterized for 1 mM, 5 mM, and 10 mM glucose, then thoroughly washed with a phosphate buffered saline solution and tested again. The response of the IPCCA was fully reversible, with the greatest variation in diffraction response of ± 1 nm for the addition of 1 mM glucose, which is three times less than the variation in average diffraction wavelength response observed for three separate IPCCA exposed to 1 mM glucose. (Lines are added to aid the eye.)

It was previously shown that the use of filler molecules can enable reversible dehydration of hydrogels[95-97]. We recently demonstrated that Ni^{+2}-sensitive PCCA, affixed to a gel-stabilizing sheet (Bio-rad), dried in the presence of high buffer concentrations can be reversibly rehydrated[66].
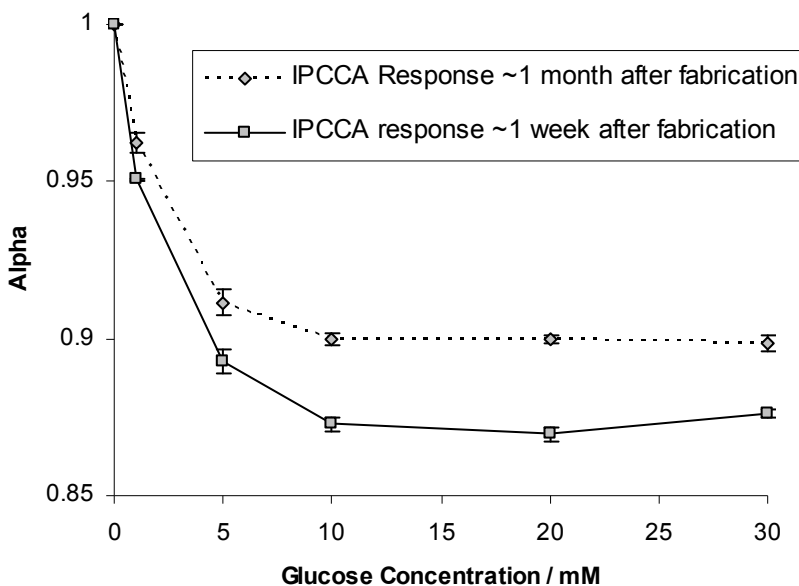
Figure 3-9. IPCCA response dependence on aqueous storage time. After storage in aqueous buffer solution for 1 month, the average response of the IPCCA to 20 mM glucose is decreased by ~23%. Lines are added to aid the eye.

After characterizing the sensing response of an IPCCA to various concentrations of glucose, we exposed it to a concentrated glucose solution (~45 wt %) for 30 min., and then allowed it to air dry. The hydrogel diffraction blue-shifted, but continued to diffract upon drying, which indicates that the ordering of the embedded CCA was maintained during dehydration. The hydrogel was rehydrated, rinsed thoroughly in PBS, and then the sensing response was characterized. As shown in Figure 3-10, the sensing ability of the material was

retained, with a ~24% increase in sensitivity between glucose concentrations of 1 mM and 5 mM.
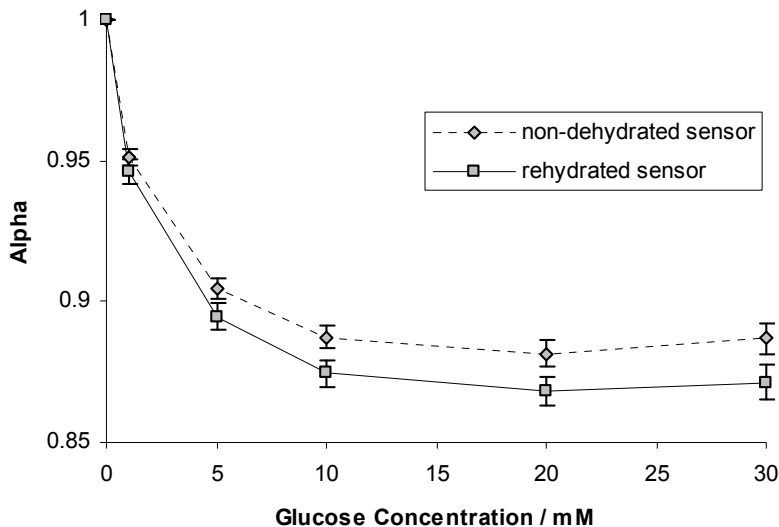
Figure 3-10. IPCCA response dependence on rehydration. The IPCCA retains sensing capability after drying in the presence of a concentrated glucose solution. The weight percent of glucose is sufficient to prevent the irreversible collapse of the acrylamide hydrogel network. The increase in spectral response after rehydration is due to the liberation of previously inaccessible BA sites during the "conditioning step" of equilibration in 45 wt% glucose. (Lines are added to aid the eye.)

We attribute this increased sensitivity upon rehydration to processes which occur upon the exposure of the IPCCA to the highly concentrated glucose solution prior to dehydration. Although the total concentration of BA sites within the hydrogel remains relatively constant, the number of accessible sites is increased by this "conditioning" step. When the IPCCA is exposed to the highly concentrated glucose solution in pure water, the hydrogel swells significantly, owing to the high concentration of charged 1:1 complex sites within the hydrogel and the

resulting Donnan potential. We postulate that this exercise in hydrogel volume, along with the high concentration of glucose in solution, liberates previously buried BA binding sites within the hydrogel. The increased accessibility of these additional sites results in an increased spectral response of the hydrogel sensing material after rehydration.

Using the average starting diffraction (when the glucose concentration is zero) of three separate runs for both the original IPCCA and the rehydrated IPCCA, we observe an ~8 nm decrease in initial diffraction after rehydration, which indicates that, when dried in the presence of a concentrated glucose solution, our IPCCA material reswells to ~97% of its initial volume.

The high concentration of glucose in the drying solution the IPCCA was exposed to prevents the irreversible and inhomogeneous collapse of the porous acrylamide hydrogel network. The excess glucose is easily removed from the material upon rehydration. The natural occurrence of glucose in bodily fluids, combined with the small required size of sensing material (1 mm x 1 mm) for optrode construction and therefore minuscule amount of glucose released upon rehydration within those fluids, makes it a logical choice for a filler molecule for use *in vivo*. The reversible rehydration of our glucose-stabilized IPCCA increases the potential for successful IPCCA commercialization.

3.4   CONCLUSIONS

We modified the synthesis and fabrication of our photonic crystal hydrogel glucose sensors to enable the monitoring of high concentrations of glucose, such as found in blood. This material is reproducibly fabricated and senses glucose reversibly over a period of one week. We demonstrate conditions which allow the sensor to be dried and rehydrated while retaining its

diffraction and sensing properties. We significantly increased our understanding of the IPCCA sensing mechanism, by modeling the response using independently determined effective crosslink concentrations in the hydrogel as well as the independently measured glucose association constant of the 5-amino-2-fluorophenylboronic acid derivative used in the sensor.

3.5 ACKNOWLEDGEMENTS

3.6 REFERENCES

(1) Cakir, M.; Altunbas, H.; Karayalcin, U. *J. Clin. Endocrinol. Metab.* **2003**, *88*, 1402-1402.

(2) Palacio, A.; Smiley, D.; Ceron, M.; Klein, R.; Cho, I. S.; Mejia, R.; Umpierrez, G. E. *J. Hosp. Med.* **2008**, *3*, 212-217.

(3) Capes, S. E.; Hunt, D.; Malmberg, K.; Gerstein, H. C. *Lancet* **2000**, *355*, 773-778.

(4) Smiley, D. D.; Umpierrez, G. E. *South. Med. J.* **2006**, *99*, 580-589.

(5) Conner, T. M.; Flesner-Gurley, K. R.; Barner, J. C. *Ann. Pharmacother.* **2005**, *39*, 492-501.

(6) Estrada, C. A.; Young, J. A.; Nifong, L. W.; Chitwood, W. R. *Ann. Thorac. Surg.* **2003**, *75*, 1392-1399.

(7) Krinsley, J. S. *Mayo Clin. Proc.* **2003**, *78*, 1471-1478.

(8) Garg, R.; Bhutani, H.; Alyea, E.; Pendergrass, M. *Diabetes Care* **2007**, *30*, 993-994.

(9) Matz, K.; Keresztes, K.; Tatschl, C.; Nowotny, M.; Dachenhausenm, A.; Brainin, M.; Tuomilehto, J. *Diabetes Care* **2006**, *29*, 792-797.

(10) Jeremitsky, E.; Omert, L. A.; Dunham, C. M.; Wilberger, J.; Rodriguez, A. *J. Trauma* **2005**, *58*, 47-50.

(11) Ahmann, A. *Endocr. Pract.* **2004**, *10 Suppl 2*, 53-56.

(12) American Diabetes Association, *Total Prevalence of Diabetes & Pre-diabetes*, 2008.

(13) Aro, S.; Kangas, T.; Reunanen, A.; Salinto, M.; Koivisto, V. *Diabetes Care* **1994**, *17*, 1320-1329.

(14) Naslafkih, A.; Sestier, F. *J. Insur. Med.* **2003**, *35*, 102-113.

(15) Ahmann, A. *Endocrinologist* **1998**, *8*, 250-259.

(16) Hirsch, I. B.; Paauw, D. S.; Brunzell, J. *Diabetes Care* **1995**, *18*, 870-878.

(17) McCowen, K. C.; Malhotra, A.; Bistrian, B. R. *Crit. Care Clin.* **2001**, *17*, 107-124.

(18) Mizock, B. A. *Am. J. Med.* **1995**, *98*, 75-84.

(19) *Diabetes Care* **2008**, *31*, S5-S11.

(20) Schmeltz, L. R.; DeSanti, A. J.; Thiyagarajan, V.; Schmidt, K.; O'Shea-Mahler, E.; Johnson, D.; Henske, J.; McCarthy, P. M.; Gleason, T. G.; McGee, E. C.; Molitch, M. E. *Diabetes Care* **2007**, *30*, 823-828.

(21) Van den Berghe, G.; Wilmer, A.; Hermans, G.; Meersseman, W.; Wouters, P. J.; Milants, I.; Van Wijngaerden, E.; Bobbaers, H.; Bouillon, R. *N. Engl. J. Med.* **2006**, *354*, 449-461.

(22) Krinsley, J. S. *Mayo Clin. Proc.* **2004**, *79*, 992-1000.

(23) Krinsley, J. S.; Jones, R. L. *Chest* **2006**, *129*, 644-650.

(24) Van den Berghe, G. *J. Clin. Invest.* **2004**, *114*, 1187-1195.

(25) Eggert, H.; Frederiksen, J.; Morin, C.; Norrild, J. C. *J. Org. Chem.* **1999**, *64*, 3846-3852.

(26) Lorand, J. P.; Edwards, J. O. *J. Org. Chem.* **1959**, *24*, 769-774.

(27) Fang, H.; Kaur, G.; Wang, B. H. *J. Fluoresc.* **2004**, *14*, 481-489.

(28) James, T. D.; Sandanayake, K.; Shinkai, S. *Supramol. Chem.* **1995**, *6*, 141-157.

(29) James, T. D.; Shinkai, S. *Top. Curr. Chem.* **2002**, *218*, 159-200.

(30) Schneider, H. J.; Kato, K.; Strongin, R. M. *Sensors* **2007**, *7*, 1578-1611.

(31) Wang, W.; Gao, X. M.; Wang, B. H. *Curr. Org. Chem.* **2002**, *6*, 1285-1317.

(32) James, T. D. In *Creative Chemical Sensor Systems*, 2007; Vol. 277, 107-152.

(33) Kondepati, V. R.; Heise, H. M. *Anal. Bioanal. Chem.* **2007**, *388*, 545-563.

(34) Park, S.; Boo, H.; Chung, T. D. *Anal. Chim. Acta* **2006**, *556*, 46-57.

(35) Hovorka, R. *Diabet. Med.* **2006**, *23*, 1-12.

(36) Striegler, S. *Curr. Org. Chem.* **2003**, *7*, 81-102.

(37) James, T. D.; Sandanayake, K.; Shinkai, S. *Angew. Chem.* **1996**, *35*, 1911-1922.

(38) James, T. D. In *Boronic Acids*; Hall, D. G., Ed., 2005, 441-479.

(39) Badugu, R.; Lakowicz, J. R.; Geddes, C. D. *J. Fluoresc.* **2004**, *14*, 617-633.

(40) Shinkai, S.; Takeuchi, M. *Biosens. Bioelectron.* **2004**, *20*, 1250-1259.

(41) Ferrier, R. J. *Adv. Carbohydr. Chem. Biochem.* **1978**, *35*, 31-80.

(42) Springsteen, G.; Wang, B. *Tetrahedron* **2002**, *58*, 5291-5300.

(43) Alexeev, V. L.; Das, S.; Finegold, D. N.; Asher, S. A. *Clin. Chem.* **2004**, *50*, 2353-2360.

(44) Alexeev, V. L.; Sharma, A. C.; Goponenko, A. V.; Das, S.; Lednev, I. K.; Wilcox, C. S.; Finegold, D. N.; Asher, S. A. *Anal. Chem.* **2003**, *75*, 2316-2323.

(45) Ben-Moshe, M.; Alexeev, V. L.; Asher, S. A. *Anal. Chem.* **2006**, *78*, 5149-5157.

(46)   Asher, S. A.; Alexeev, V. L.; Goponenko, A. V.; Sharma, A. C.; Lednev, I. K.; Wilcox, C. S.; Finegold, D. N. *J. Am. Chem. Soc.* **2003**, *125*, 3322-3329.

(47)   Asher, S. A.; Alexeev, V. L.; Lednev, I. K.; Sharma, A. C.; Wilcox, C. US Patent 2003027240, 2003.

(48)   Asher, S. A.; Holtz, J. H. US Patent 5854078, 1998.

(49)   Asher, S. A.; Holtz, J. H. WO Patent 9819787, 1998.

(50)   Asher, S. A.; Holtz, J. H. WO Patent 9841859, 1998.

(51)   Holtz, J. H.; Holtz, J. S. W.; Munro, C. H.; Asher, S. A. *Anal. Chem.* **1998**, *70*, 780-791.

(52)   Holtz, J. H.; Asher, S. A. *Nature* **1997**, *389*, 829-832.

(53)   Sunkara, H. B.; Weissman, J. M.; Penn, B. G.; Frazier, D. O.; Asher, S. A. *Polym. Prepr.* **1996**, *37*, 453-454.

(54)   Asher, S. A.; Holtz, J.; Liu, L.; Wu, Z. *J. Am. Chem. Soc.* **1994**, *116*, 4997-4998.

(55)   Tikhonov, A.; Coalson, R. D.; Asher, S. A. *Phys. Rev. B* **2008**, *77*, 235404/235401-235404/235416.

(56)   Asher, S. A.; Weissman, J. M.; Tikhonov, A.; Coalson, R. D.; Kesavamoorthy, R. *Phys. Rev. E* **2004**, *69*, 066619/066611-066619/066614.

(57)   Reese, C. E.; Guerrero, C. D.; Weissman, J. M.; Lee, K.; Asher, S. A. *J. Colloid Interface Sci.* **2000**, *232*, 76-80.

(58)   Asher, S. A.; Holtz, J.; Weissman, J.; Pan, G. *MRS Bulletin* **1998**, *23*, 44-50.

(59)   Asher, S. A. EP Patent 168988, 1986.

(60)   Flaugh, P. L.; O'Donnell, S. E.; Asher, S. A. *Appl. Spectrosc.* **1984**, *38*, 847-850.

(61)   Carlson, R. J.; Asher, S. A. *Appl. Spectrosc.* **1984**, *38*, 297-304.

(62) Rundquist, P. A.; Photinos, P.; Jagannathan, S.; Asher, S. A. *J. Chem. Phys.* **1989**, *91*, 4932-4941.

(63) Reese, C. E.; Asher, S. A. *Anal. Chem.* **2003**, *75*, 3915-3918.

(64) Asher, S. A.; Sharma, A. C.; Goponenko, A. V.; Ward, M. M. *Anal. Chem.* **2003**, *75*, 1676-1683.

(65) Asher, S. A.; Peteu, S. F.; Reese, C. E.; Lin, M. X.; Finegold, D. *Anal. Bioanal. Chem.* **2002**, *373*, 632-638.

(66) Baca, J. T.; Finegold, D. N.; Asher, S. A. *Analyst* **2008**, *133*, 385-390.

(67) Kimble, K. W.; Walker, J. P.; Finegold, D. N.; Asher, S. A. *Anal. Bioanal. Chem.* **2006**, *385*, 678-685.

(68) Sharma, A. C.; Jana, T.; Kesavamoorthy, R.; Shi, L.; Virji, M. A.; Finegold, D. N.; Asher, S. A. *J. Am. Chem. Soc.* **2004**, *126*, 2971-2977.

(69) Xu, X.; Goponenko, A. V.; Asher, S. A. *J. Am. Chem. Soc.* **2008**, *130*, 3113-3119.

(70) Lee, K.; Asher, S. A. *J. Am. Chem. Soc.* **2000**, *122*, 9534-9537.

(71) Walker, J. P.; Kimble, K. W.; Asher, S. A. *Anal. Bioanal. Chem.* **2007**, *389*, 2115-2124.

(72) Walker, J. P.; Asher, S. A. *Anal. Chem.* **2005**, *77*, 1596-1600.

(73) Baca Justin, T.; Finegold David, N.; Asher Sanford, A. *Ocul. Surf.* **2007**, *5*, 280-293.

(74) Burtis, C. A., Ashwood, E. R., Eds. *Tietz Textbook of Clinical Chemistry, 3rd Edition*; W. B. Saunders: Philadelphia, 1999.

(75) Springsteen, G.; Wang, B. *Chem. Commun.* **2001**, 1608-1609.

(76) Dowlut, M.; Hall, D. G. *J. Am. Chem. Soc.* **2006**, *128*, 4226-4227.

(77) Flory, P. J. *Principles of Polymer Chemistry;* Cornell University Press: Ithaca, 1953.

(78)   Erman, B.; Mark, J. E. *Structures and Properties of Rubberlike Networks*, Oxford
         University Press: New York, 1997.

(79)   Connors, K. A. *Binding Constants: The Measurements of Molecular Complex Stability*,
         John Wiley & Sons, Inc.: New York, 1987.

(80)   Gray, C. W.; Houston, T. A. *J. Org. Chem.* **2002**, *67*, 5426-5428.

(81)   Sartain, F. K.; Yang, X. P.; Lowe, C. R. *Anal. Chem.* **2006**, *78*, 5664-5670.

(82)   Wiskur, S. L.; Lavigne, J. L.; Metzger, A.; Tobey, S. L.; Lynch, V.; Anslyn, E. V. *Chem-
         Eur. J.* **2004**, *10*, 3792-3804.

(83)   Yang, X. P.; Lee, M. C.; Sartain, F.; Pan, X. H.; Lowe, C. R. *Chem-Eur. J.* **2006**, *12*,
         8491-8497.

(84)   Babcock, L.; Pizer, R. *Inorg. Chem.* **1980**, *19*, 56-61.

(85)   Friedman, S.; Pace, B.; Pizer, R. *J. Am. Chem. Soc.* **1974**, *96*, 5381-5384.

(86)   Neglia, C. I.; Cohen, H. J.; Garber, A. R.; Ellis, P. D.; Thorpe, S. R.; Baynes, J. W. *J.
         Biol. Chem.* **1983**, *258*, 4279-4283.

(87)   Day, J. F.; Thorpe, S. R.; Baynes, J. W. *J. Biol. Chem.* **1979**, *254*, 595-597.

(88)   Olufemi, S.; Talwar, D.; Robb, D. A. *Clin. Chim. Acta* **1987**, *163*, 125-136.

(89)   Yatscoff, R. W.; Tevaarwerk, G. J. M.; Macdonald, J. C. *Clin. Chem.* **1984**, *30*, 446-449.

(90)   Guthrow, C. E.; Morris, M. A.; Day, J. F.; Thorpe, S. R.; Baynes, J. W. *Proc. Natl. Acad.
         Sci. U. S. A.* **1979**, *76*, 4258-4261.

(91)   Mohamadi-Nejad, A.; Moosavi-Movahedi, A. A.; Hakimelahi, G. H.; Sheibani, N. *Int. J.
         Biochem. Cell. B.* **2002**, *34*, 1115-1124.

(92)   Ikeda, K.; Sakamoto, Y.; Kawasaki, Y.; Miyake, T.; Tanaka, K.; Urata, T.; Katayama, Y.;
         Ueda, S.; Horiuchi, S. *Clin. Chem.* **1998**, *44*, 256-263.

(93)   Okayama, H.; Ueda, K.; Hayaishi, O. *Proc. Natl. Acad. Sci. U. S. A.* **1978**, *75*, 1111-1115.

(94)   Weith, H. L.; Wiebers, J. L.; Gilham, P. T. *Biochemistry* **1970**, *9*, 4396-4401.

(95)   Allen, R. C. US Patent 5159049, 1992.

(96)   Allen, R. C.; Radola, B. J. US Patent 4746551, 1988.

(97)   Fang, T.-Y. WO Patent 9719989, 1997.

4.0 DEPENDENCE OF PHOTONIC CRYSTAL NANOCOMPOSITE ELASTICITY ON CRYSTALLINE COLLOIDAL ARRAY PARTICLE SIZE

Ward Muscatello, M. M.; Stunja, L.E.; Thareja, P.; Wang, L.; Bohn, J.J.; Velankar, S.S.; Asher, S.A.; *submitted to Nano Letters,* **2008**.

We determined the dependence of the elastic shear storage modulus for our photonic crystal hydrogels, which embed crystalline colloidal arrays of non-close-packed particles, on their incorporated nanoparticle size and polymerization conditions. The modulus increases linearly with increasing nanoparticle diameters, due to slippage of the hydrogel matrix at the particle surfaces. The effective crosslink densities, calculated from the storage moduli, indicate we can affect the responsivity of our materials by controlling the included nanoparticle size.

4.1 INTRODUCTION

The properties of hydrogel materials depend on their network structure, which is determined predominantly by the hydrogel polymer volume fraction and the degree of hydrogel crosslinking[1-3]. In an effort to optimize the utility of our photonic crystal hydrogel materials, and to improve our understanding of these systems, we investigated the mechanical properties of

79

these photonic crystal hydrogels as a function of polymerization conditions and prepolymerization solution compositions.
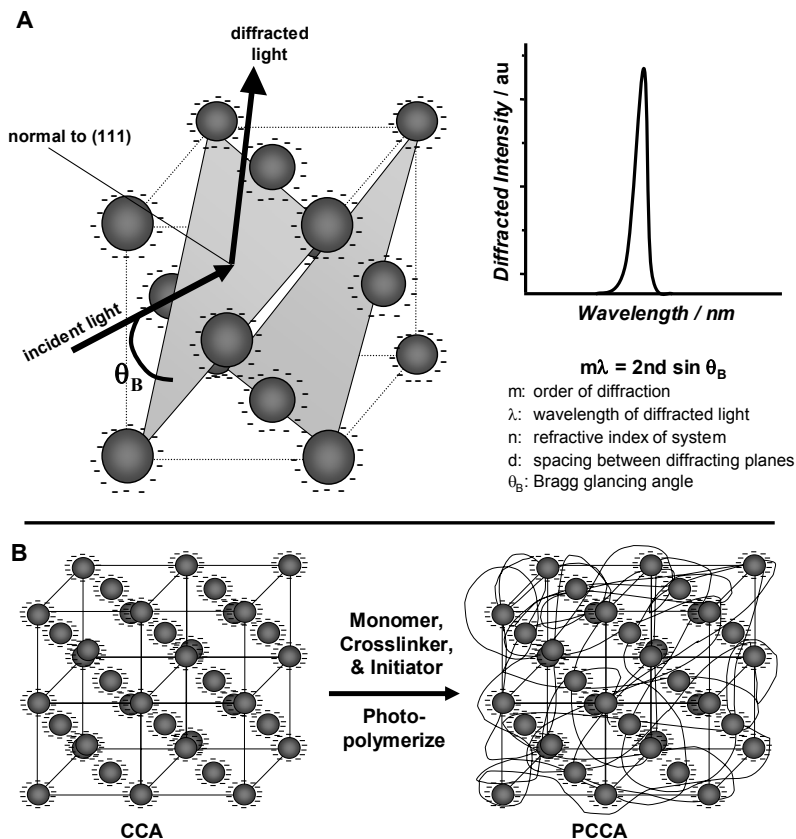
Figure 4-1. (A) Crystalline Colloidal Arrays (CCA) form due to the electrostatic repulsion between the highly charged, monodisperse polystyrene particles. The spacing between particles is such that they diffract visible light according to Bragg's law. (B) Polymerized Crystalline Colloidal Arrays (PCCA) are formed by polymerizing a hydrogel network around the CCA.

Our photonic crystal hydrogel materials contain mesoscopically periodic arrays of colloidal particles that self-assemble into highly-ordered crystalline colloidal arrays (CCA), with lattice spacings that Bragg diffract visible light (Figure 4-1A)[4-11]. The CCA are polymerized

within hydrogels forming a polymerized CCA (PCCA) (Figure 4-1B)[12]. These PCCA optically report on volume changes experienced by the hydrogels, since the observed diffraction wavelength directly depends upon the spacing between lattice planes. These PCCA have been used for chemical sensing by functionalizing them such that changes in the concentration of the analyte of interest actuate changes in the PCCA volume and, thereby, the diffraction wavelength[13-18]. Intelligent PCCA (IPCCA) have been developed for the detection of multiple analytes, including glucose[19-23], cations[24-28], ammonia[29], pH[30,31], organophosphates[32,33], and creatinine[34].

The viscoelastic properties of a hydrogel are predominantly determined by the hydrogel network structure[1,3]. In the work here we develop new insight into this network structure by oscillatory shear rheometry measurements, which characterize the PCCA shear storage modulus. This modulus monitors the effective crosslink density of the PCCA hydrogels[1,3]. The effective crosslink density is derived from normal hydrogel crosslinks, as well as from interactions of the hydrogel network with the embedded CCA particles.

In spite of the numerous studies that examined the impact of nanoparticle inclusions on elastomer mechanical properties, there still remains significant quantitative disagreement on the dependence of these properties on nanoparticle size[1,3,35-51]. We present here the first definitive study of how the mechanical properties of a swollen hydrogel depend upon the diameter of nonbonded embedded nanoparticles.

4.2 RESULTS AND DISCUSSION

4.2.1 Effect of Particle Size on Storage Modulus

Monodisperse, highly charged polystyrene colloidal particles with diameters between 114-186 nm were used in the preparation of the PCCA studied (Table 4-1). All of these colloids readily formed CCA, which exhibited sharp diffraction peaks in the visible region. Figure 4-2 shows a TEM micrograph of the highly charged, monodisperse 186 nm polystyrene spheres. The CCA solutions used for PCCA preparation were diluted with water to identical weight percents, to ensure constant overall polymer content within the corresponding prepolymerization solutions.

CCA diameter	CCA weight %	CCA λ_m	PCCA G'	PCCA v_e
114 nm	16.35 %	425 nm	670 Pa	0.00046 M
124 nm	16.35 %	510 nm	860 Pa	0.00059 M
145 nm	16.35 %	603 nm	1090 Pa	0.00075 M
186 nm	16.35 %	716 nm	1590 Pa	0.00109 M

Table 4-1. Polymerized Crystalline Colloidal Array shear storage moduli (G') and effective crosslink densities (v_e) as a function of CCA particle size.

Hydrogels were prepared using the different sized CCA particles and were analyzed at a constant temperature. Figure 4-3A shows the frequency dependence of the PCCA shear storage

modulus for the different size CCA particles, while Figure 4-3B shows that the modulus increases linearly with increasing CCA particle diameter.
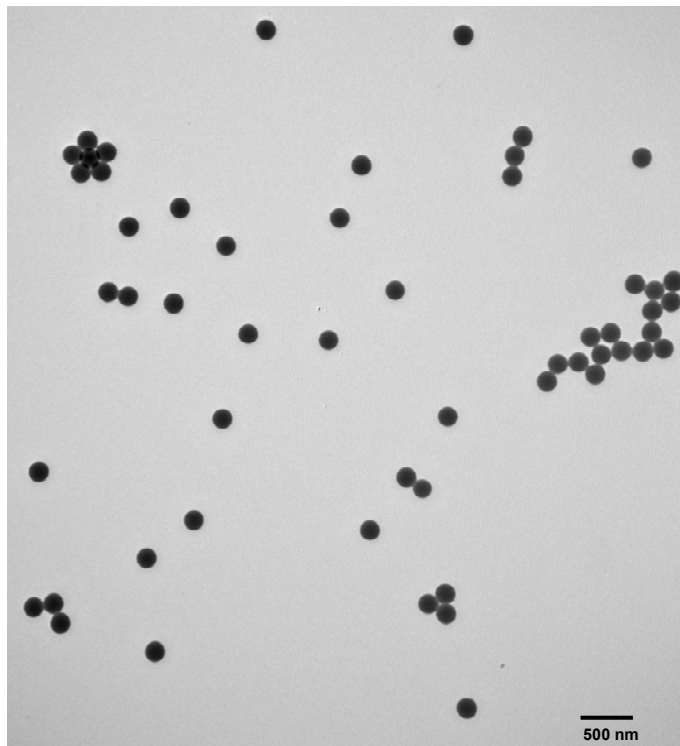
Figure 4-2. TEM of highly monodisperse, highly charged 186 nm polystyrene colloidal particles prepared via emulsion polymerization. The particle size was characterized using the IGOR Pro image processing software.

These results are somewhat surprising considering previous reports[1,3,35,38,39,43,46,47]. Filler particles are commonly utilized to improve the mechanical properties of polymers by increasing the modulus. Previous studies have shown that the extent of modulus increase depends on the particle size, with smaller particles typically giving rise to a larger modulus increase than larger particles, exactly the opposite of what we observe for our PCCA.
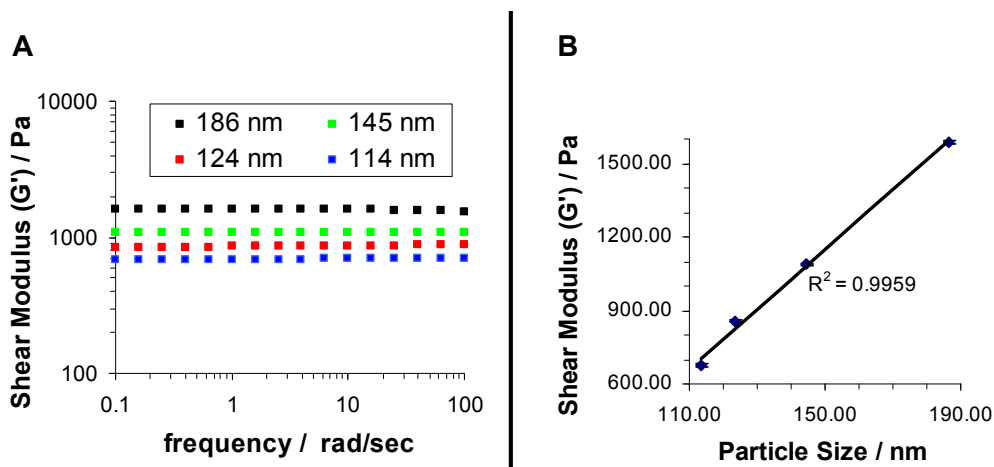
Figure 4-3. (A) The average values of the shear storage modulus (G′), for PCCA hydrogels prepared from different CCA particle sizes, as a function of angular frequency. (B) The modulus increases linearly with increasing CCA particle size, over the range of particle sizes studied.

The difference between our results and those of previous studies most likely derives from the fundamental differences in the morphologies of the systems studied. The previous studies used filler nanoparticles which were randomly dispersed and showed a tendency to aggregate[39,42]. Our nanoparticles are electrostatically stabilized, due to the high concentration of surface immobilized acid groups. The high surface charge prevents aggregation and causes the particles to self assemble into an fcc array which uniformly spans the material, as evident in the SEM of a PCCA shown in Figure 4-4A. Further, the extent of interfacial interaction between the filler particle and surrounding polymer matrix will impact the overall viscoelastic response of the material[36-44,47-49]. The fact that many CCA particles have fallen out of the surface layer of our PCCA hydrogel material (Figure 4-4B) demonstrates the lack of covalent attachment or interfacial adhesion between the polystyrene particles and the surrounding hydrogel matrix.
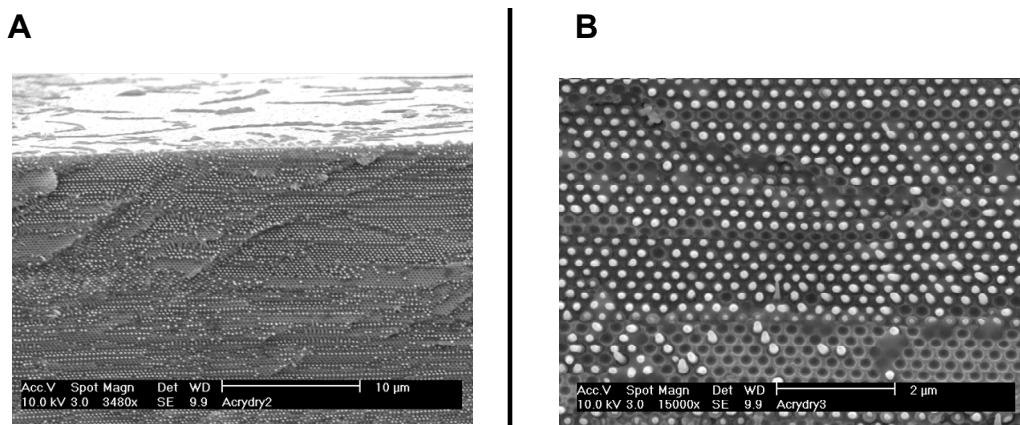
Figure 4-4. (A) SEM of PCCA hydrogel material illustrating the long range order of the embedded CCA particles. (B) Higher magnification SEM image of PCCA, illustrating the lack of interaction between the embedded particles and the surrounding polymer matrix. The particles actually "fall out" of the surface layer of the surrounding matrix upon sample preparation.

The correlation between the modulus and the particle size can be understood by treating the shear storage modulus as resulting from the contributions of three distinct regions within the PCCA. Figure 4-5A illustrates two PCCA consisting of identical colloid polymer particle volume fractions but with different diameter particles. Each particle is surrounded by a small interfacial shell, in which there are no interactions between the particle surface and the surrounding hydrogel matrix. As illustrated in Figure 4-5B, the overall modulus can be thought of as a series of connected springs. The CCA particles would contribute a very tight spring because of the large storage modulus of the rigid polystyrene particle. The hydrogel matrix would contribute a smaller force constant spring since it is more elastic than the particles. The lack of adhesion between the embedded particles and surrounding hydrogel matrix results in slip, which is equivalent to a spring with a significantly low force constant. Given a constant particle volume fraction, the PCCA containing smaller particles have a larger contribution from the

85

interfacial shell region, owing to increased surface area, giving rise to a lower overall PCCA modulus.
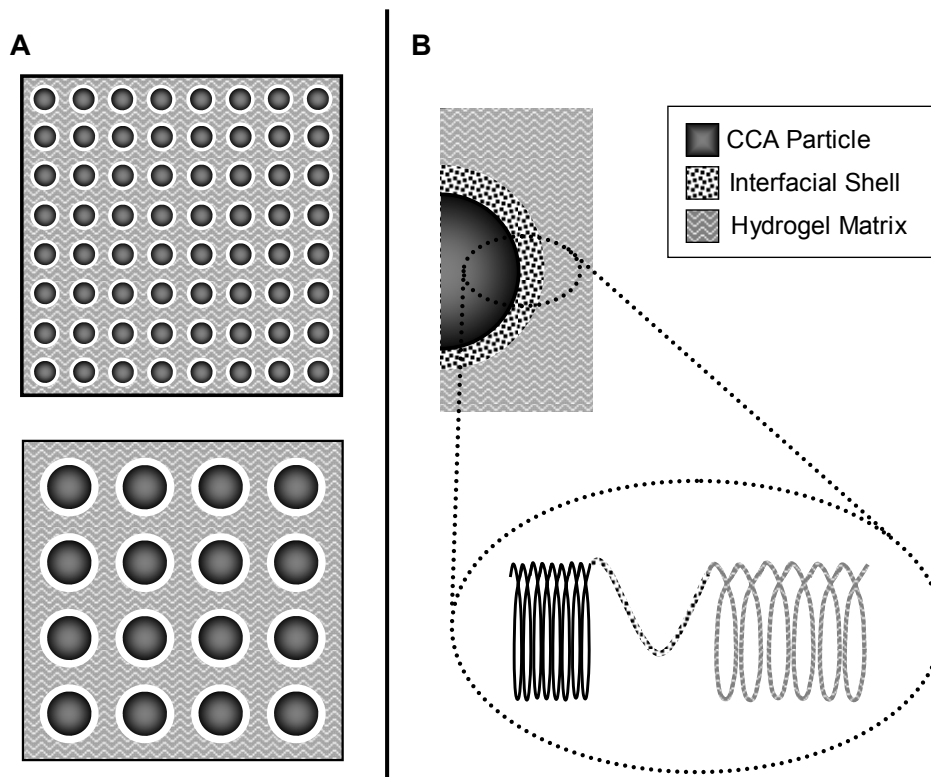
Figure 4-5. (A) Illustration of two PCCA prepared with identical polymer volume fractions but different sized CCA (B) Illustration of proposed mechanism for decreased shear modulus with decreased CCA particle diameter. The overall modulus can be thought of as a series of connected springs. The rigid CCA particles contribute a very tight spring and the surrounding hydrogel matrix contributes a smaller force constant spring as it is more elastic. The lack of adhesion between the embedded particles and surrounding hydrogel matrix, as found in the interfacial shell, results in slip which is equivalent to a spring with a very low force constant. Given a constant polymer volume fraction, the PCCA containing smaller particles have a larger contribution from the interfacial shell region, owing to increased surface area, giving rise to a lower overall PCCA storage modulus.

4.2.2 Effect of Storage Modulus Determination on IPCCA Design

Using polymer rubber theory we can determine the effective crosslink density (υ_e) from the experimentally determined shear storage modulus (G') and the polymer volume fraction (ϑ)[1]:

$$G' = \upsilon_e RT \vartheta^{\frac{1}{3}}.$$

Equation 4-1

The effective crosslink density of these constant polymer volume fraction PCCA scales with the modulus and thus increases as the particle size increases. As can be seen in Table 4-1, an increase of particle size of ~9% will result in an increase of effective crosslink density of ~28%. Since the degree of hydrogel swelling is directly related to the effective crosslink density[1-3], the responsivity of our IPCCA can be increased by utilizing smaller diameter colloidal particles.

The sensing mechanisms employed in our PCCA sensing material can be modeled by using Flory's model for the swelling of network structures[1], where the total osmotic pressure at equilibrium is considered to be the balance of osmotic pressures arising from changes in the free energy of mixing (Π_M), the elastic free energy (Π_E), and the Donnan potential (Π_{Ion}):

$$\Pi_T = \Pi_M + \Pi_E + \Pi_{Ion} = 0.$$

Equation 4-2

The osmotic pressure arising from the change in the elastic free energy is determined by the effective crosslink density of the system:

$$\Pi_{\mathrm{E}} = -\frac{\partial \Delta G_{\mathrm{E}}}{\partial V} = -RT \cdot \upsilon_e \left[\left(\frac{V_{\mathrm{m}}}{V} \right)^{1/3} - \frac{1}{2} \frac{V_{\mathrm{m}}}{V} \right],$$

Equation 4-3

where R is the universal gas constant, T is the temperature, V is the current volume of the hydrogel, and V_{m} is the volume of the relaxed hydrogel network.

The diffraction shift observed in a PCCA sensing material is directly related to the volume of the hydrogel:

$$\left(\frac{V}{V^*} \right)^{\frac{1}{3}} = \frac{\lambda}{\lambda^*},$$

Equation 4-4

where λ and λ^* are the diffracted wavelengths in the presence and absence of the analyte respectively and V and V^* are the volumes of the network in the presence and absence of the analyte of interest respectively.

Accurate determination of the effective crosslink density of our system affords capable modeling of our sensor response, providing increased understanding of our material and a more directed approach towards material development.

4.2.3   Effect of Polymerization Conditions on Storage Modulus

Hydrogels were prepared with and without embedded CCA, both in the presence and absence of oxygen. The materials moduli were analyzed at a constant temperature, and the resulting shear storage moduli are shown in Figure 4-6. As expected, hydrogels prepared in the absence of oxygen show higher moduli than those prepared with oxygen. This occurs because oxygen is known to quench free-radical polymerizations, leading to decreased monomer and

crosslinker incorporation. It is interesting to note, as well, that the effect of oxygen exclusion is more pronounced for those hydrogel materials prepared without CCA particle inclusions.
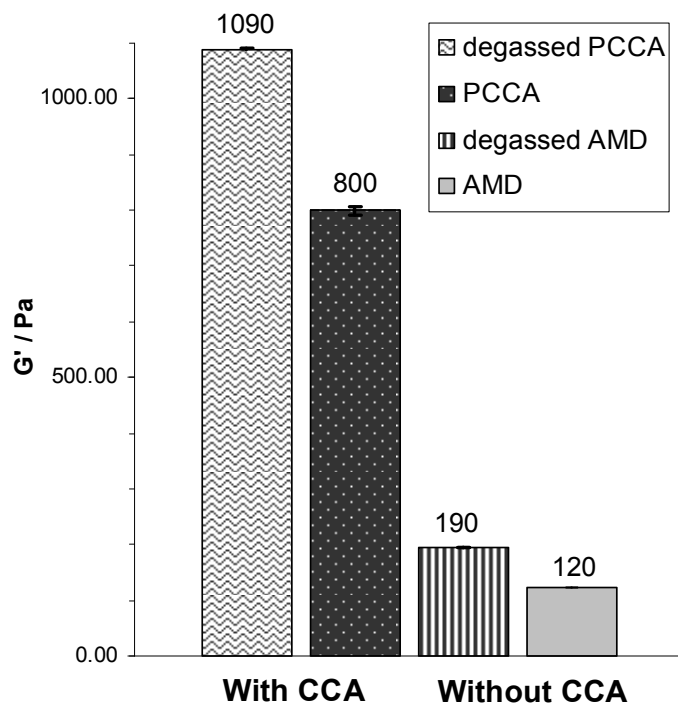
Figure 4-6. Effect of polymerization conditions on hydrogel storage moduli. Excluding oxygen (degassing) from the polymerization process increases the moduli of the PCCA and the hydrogels prepared without CCA (AMD). This effect is more pronounced for hydrogels prepared without the nanoparticle (145 nm) inclusions.

The observed strong dependence of the modulus of the PCCA on the presence of oxygen clearly indicates the importance of controlling this variable to fabricate reproducibly responsive PCCA sensors. This point is further illustrated by the fact that, in previous studies, we have observed that PCCA materials prepared in the absence of oxygen exhibit a more homogeneous

diffraction across the surface (±15 nm) as opposed to those prepared in the presence of oxygen (±30 nm).

Although the increase in the storage modulus with oxygen exclusion will result initially in a less responsive PCCA, as an increase in the effective crosslink density that scales with the modulus will result in a less swellable hydrogel material, the improved polymerization process provides better control over the crosslinker and monomer incorporation. The composition of the prepolymerization solution can be altered to produce a material with the desired swellability.

Of interest is the fact that the effective crosslink density is dominated by nanoparticle inclusions, as opposed to the BisAA crosslinker (Figure 4-6). Although the absence of a reliable molecular theory makes it difficult to determine the exact mechanism of filler reinforcement, the decreased water content and reinforcement from the embedded CCA particles in the PCCA results in a 2.5-fold increase in the effective crosslink density compared to that of hydrogels prepared without nanoparticle inclusions. The rigid CCA particles deform less than the surrounding polymer matrix, causing the material strain to be reduced overall[1,3,52]. In addition, the volume occupied by the filler particles will effect the polymer chain distribution during polymerization and the resulting polymer chain mobility within the elastomer[3]. The modulus values for our composite material are reasonable considering values reported for other highly swollen hydrogels[2,50,51,53-56]. Further investigation of the PCCA modulus dependence on CCA, monomer, and crosslinker concentrations is currently underway in our laboratory.

4.3   CONCLUSIONS

We characterized the storage modulus, and thereby effective crosslink density, of our photonic crystal hydrogel material as a function of incorporated CCA particle size and polymerization conditions.   We have found that the storage modulus increases linearly with increasing particle size.   We attribute the decrease of the overall modulus with decreasing particle size to the increased contribution of slip within the system, owing to the increased surface area of smaller particles.   We also found that the storage modulus increases upon exclusion of oxygen during polymerization, and that this increase is more pronounced for hydrogels without CCA inclusions.   We have increased our understanding of PCCA materials, providing for a more directed approach to improved PCCA sensor material development, as the degree of swelling of the hydrogel material is directly related to the effective crosslink density.

4.4   EXPERIMENTAL

4.4.1   Materials

2,2-diethoxyacetophenone (DEAP, 98%, Acros Organics), acrylamide (98%, AA, Sigma), N,N'-methylenebisacrylamide (98%, BisAA, Sigma), and dimethyl sulfoxide (DMSO, Fisher) were all used as received.   Deionized water (Barnstead Nanopure Water Purification System) was used for solution preparation.

4.4.2 CCA Preparation

Monodisperse, highly-charged polystyrene spheres were prepared via emulsion polymerization as reported elsewhere[6], with additional initiator and charged monomer being added near the end of the polymerization process. The colloidal particles were cleaned via dialysis against deionized water and were subsequently shaken with ion-exchange resin.

4.4.3 PCCA Hydrogel Preparation

The PCCA studied were synthesized by UV-initiated free radical polymerization. In a typical recipe, 0.1 g AA, 0.002 g BisAA, ion-exchange resin, and 2.0 g CCA were vortexed together in a small glass vial. The vial was wrapped in Al foil and 20 μL of DEAP (20 % in DMSO) were added. The solution was vortexed again. The prepolymerization solution, polymerization cell (two quartz plates separated by a 250 μm parafilm spacer), and necessary equipment (Ziploc bag, plastic syringes and needle tips, and centrifuge tube) were degassed in a vacuum chamber and then blanketed with nitrogen within a glove bag. Within the glove bag, the polymerization solution was centrifuged, injected into the cell, and then sealed within a Ziploc bag, so as to preserve the nitrogen environment during polymerization. The cell was exposed to UV light from two Blak-Ray (365 nm) mercury lamps to initiate the polymerization. The resulting PCCA was rinsed with large quantities of pure water. The samples were stored in deionized water until ready for testing.

For samples prepared in the presence of oxygen, the procedure followed omitted the degassing step and use of the Ziploc bag during polymerization. For samples prepared without colloid, 2 g of deionized water was used in place of the 2 g CCA solution.

4.4.4 CCA / PCCA Characterization

CCA particle sizes were measured by using transmission electron microscopy (TEM; Zeiss EM 902A) and the IGOR Pro image processing software (WaveMetrics, Inc). Optical diffraction measurements were conducted at a fixed 90° glancing angle utilizing an Ocean Optics USB2000-UV-VIS Spectrometer, a LS-1 Tungsten Halogen Light Source, and an R-series Fiber Optic Reflection Probe. PCCA were sputter coated with Pd and imaged in a Phililps FEG XL-30 field emission scanning electron microscope (SEM) operating at 10 keV.

4.4.5 PCCA Mechanical Analysis

Oscillatory shear measurements were performed with an AR2000 Rheometer (TA Instruments) using a 25 mm parallel plate geometry, with the temperature being maintained at 25 ^{o}C by a Peltier stage. After loading the sample, water was added around the edge of the sample to prevent evaporation of the water in the hydrogel during the experiment. Mechanical properties were measured using a frequency-sweep between 0.1 to 100 rad/s at a fixed oscillatory shear strain of 5%. As the material was analyzed at low strains, no further modification of the stage was necessary to prevent slip of the material.

4.6 REFERENCES

(1) Flory, P. J., *Principles of Polymer Chemistry*. Cornell University Press: New York, 1953.

(2) Anseth, K. S.; Bowman, C. N.; Brannon-Peppas, L., *Biomaterials* **1996,** *17*, (17), 1647-1657.

(3) Erman, B.; Mark, J. E., *Structures and Properties of Rubberlike Networks*. Oxford University Press: New York, 1997.

(4) Tikhonov, A.; Coalson, R. D.; Asher, S. A., *Phsy. Rev. B* **2008,** *77*, (23), 235404/1-235404/16.

(5) Asher, S. A.; Weissman, J. M.; Tikhonov, A.; Coalson, R. D.; Kesavamoorthy, R., *Phys. Rev. E* **2004,** *69*, (6-2), 066619/1-066619/14.

(6) Reese, C. E.; Guerrero, C. D.; Weissman, J. M.; Lee, K.; Asher, S. A., *J. Colloid Interface Sci.* **2000,** *232*, (1), 76-80.

(7) Asher, S. A.; Holtz, J.; Weissman, J.; Pan, G., *MRS Bulletin* **1998,** *23*, (10), 44-50.

(8) Asher, S. A., EP Patent 168988, 1986.

(9) Carlson, R. J.; Asher, S. A., *Appl. Spectrosc.* **1984,** *38*, (3), 297-304.

(10) Flaugh, P. L.; O'Donnell, S. E.; Asher, S. A., *Appl. Spectrosc.* **1984,** *38*, (6), 847-50.

(11) Rundquist, P. A.; Photinos, P.; Jagannathan, S.; Asher, S. A., *J. Chem. Phys.* **1989,** *91*, (8), 4932-41.

(12) Asher, S. A.; Holtz, J.; Liu, L.; Wu, Z., *J. Am. Chem. Soc.* **1994,** *116*, (11), 4997-8.

(13)   Asher, S. A.; Holtz, J. H., US Patent 5854078, 1998.

(14)   Asher, S. A.; Holtz, J. H., WO Patent 9819787, 1998.

(15)   Asher, S. A.; Holtz, J. H., WO Patent 9841859, 1998.

(16)   Holtz, J. H.; Holtz, J. S. W.; Munro, C. H.; Asher, S. A., *Anal. Chem.* **1998,** *70*, (4), 780-
        791.

(17)   Sunkara, H. B.; Weissman, J. M.; Penn, B. G.; Frazier, D. O.; Asher, S. A., *Polym. Prepr.*
        1996, *37*, (1), 453-4.

(18)   Holtz, J. H.; Asher, S. A., *Nature* **1997,** *389*, (6653), 829-832.

(19)   Alexeev, V. L.; Das, S.; Finegold, D. N.; Asher, S. A., *Clin. Chem.* **2004,** *50*, (12), 2353-
        2360.

(20)   Alexeev, V. L.; Sharma, A. C.; Goponenko, A. V.; Das, S.; Lednev, I. K.; Wilcox, C. S.;
        Finegold, D. N.; Asher, S. A., *Anal. Chem.* **2003,** *75*, (10), 2316-2323.

(21)   Ben-Moshe, M.; Alexeev, V. L.; Asher, S. A., *Anal. Chem.* **2006,** *78*, (14), 5149-5157.

(22)   Asher, S. A.; Alexeev, V. L.; Goponenko, A. V.; Sharma, A. C.; Lednev, I. K.; Wilcox,
        C. S.; Finegold, D. N., *J. Am. Chem. Soc.* **2003,** *125*, (11), 3322-3329.

(23)   Asher, S. A.; Alexeev, V. L.; Lednev, I. K.; Sharma, A. C.; Wilcox, C., US Patent
        2003027240, 2003.

(24)   Muscatello, M. M. W.; Asher, S. A., *Adv. Funct. Mater.* **2008,** *18*, (8), 1186-1193.

(25)   Reese, C. E.; Asher, S. A., *Anal. Chem.* **2003,** *75*, (15), 3915-3918.

(26)   Asher, S. A.; Sharma, A. C.; Goponenko, A. V.; Ward, M. M., *Anal. Chem.* **2003,** *75*, (7),
        1676-1683.

(27)   Asher, S. A.; Peteu, S. F.; Reese, C. E.; Lin, M. X.; Finegold, D., *Anal. Bioanal.Chem.*
        2002, *373*, (7), 632-638.

(28) Baca, J. T.; Finegold, D. N.; Asher, S. A., *Analyst* **2008,** *133*, (3), 385-390.

(29) Kimble, K. W.; Walker, J. P.; Finegold, D. N.; Asher, S. A., *Anal. Bioanal.Chem.* **2006,** *385*, (4), 678-685.

(30) Lee, K.; Asher, S. A., *J. Am. Chem. Soc.* **2000,** *122*, (39), 9534-9537.

(31) Xu, X.; Goponenko, A. V.; Asher, S. A., *J. Am. Chem. Soc.* **2008,** *130*, (10), 3113-3119.

(32) Walker, J. P.; Asher, S. A., *Anal. Chem.* **2005,** *77*, (6), 1596-1600.

(33) Walker, J. P.; Kimble, K. W.; Asher, S. A., *Anal. Bioanal.Chem.* **2007,** *389*, (7-8), 2115-2124.

(34) Sharma, A. C.; Jana, T.; Kesavamoorthy, R.; Shi, L.; Virji, M. A.; Finegold, D. N.; Asher, S. A., *J. Am. Chem. Soc.* **2004,** *126*, (9), 2971-2977.

(35) Zeng, X. F.; Wang, W. Y.; Wang, G. Q.; Chen, J. F., *J. Mat. Sci.* **2008,** *43*, (10), 3505-3509.

(36) Ozmusul, M. S.; Picu, R. C., *Polym. Composite* **2002,** *23*, (1), 110-119.

(37) Shi, D.; Yu, W.; Li, R. K. Y., *J. Mater. Sci.* **2008,** *43*, (3), 1162-1165.

(38) Ji, X. L.; Jing, J. K.; Jiang, W.; Jiang, B. Z., *Polym. Eng. Sci.* **2002,** *42*, (5), 983-993.

(39) Osman, M. A.; Atallah, A., *Polymer* **2006,** *47*, (7), 2357-2368.

(40) Paul, D. R.; Robeson, L. M., *Polymer* **2008,** *49*, (15), 3187-3204.

(41) Zeng, Q. H.; Yu, A. B.; Lu, G. Q., *Prog. Polym. Sci.* **2008,** *33*, (2), 191-269.

(42) Zoukrami, F.; Haddaoui, N.; Vanzeveren, C.; Sclavons, M.; Devaux, J., *Polym. Int.* **2008,** *57*, (5), 756-763.

(43) Sarvestani, A. S.; He, X.; Jabbari, E., *Biopolymers* **2007,** *85*, (4), 370-378.

(44) Hernandez, R.; Sarafian, A.; Lopez, D.; Mijangos, C., *Polymer* **2004,** *45*, (16), 5543-5549.

(45)   Thevenot, C.; Khoukh, A.; Reynaud, S.; Desbrieres, J.; Grassl, B., *Soft Matter* **2007,** *3*, (4), 437-447.

(46)   Baji, A.; Wong, S.-C.; Liu, T.; Li, T.; Srivatsan, T. S., *J. Bio. Mat. Res. B* **2007,** *81B*, (2), 343-350.

(47)   Robertson, C. G.; Lin, C. J.; Rackaitis, M.; Roland, C. M., *Macromolecules* **2008,** *41*, (7), 2727-2731.

(48)   Balazs, A. C.; Emrick, T.; Russell, T. P., *Science* **2006,** *314*, (5802), 1107-1110.

(49)   Kausch, H. H.; Michler, G. H., *J. Appl. Polym. Sci.* **2007,** *105*, (5), 2577-2587.

(50)   Foulger, S. H.; Jiang, P.; Lattam, A. C.; Smith, D. W., Jr.; Ballato, J., *Langmuir* **2001,** *17*, (19), 6023-6026.

(51)   Yanagioka, M.; Frank, C. W., *Macromolecules* **2008,** *41*, (14), 5441-5450.

(52)   McCrum, N. G.; Buckley, C. P.; Bucknall, C. B., *Principles of Polymer Engineering, 2nd Edition*. Oxford University Press: New York, 1997.

(53)   Meyvis, T. K. L.; Stubbe, B. G.; Van Steenbergen, M. J.; Hennink, W. E.; De Smedt, S. C.; Demeester, J., *Int. J. Pharm.* **2002,** *244*, (1-2), 163-168.

(54)   Quintana, J. R.; Valderruten, N. E.; Katime, I., *J. Appl. Polym. Sci.* **2002,** *85*, (12), 2540-2545.

(55)   Lopatin, V. V.; Askadskii, A. A.; Peregudov, A. S.; Vasil'ev, V. G., *J. Appl. Polym. Sci.* **2005,** *96*, (4), 1043-1058.

(56)   Dubrovskii, S. A.; Rakova, G. V., *Macromolecules* **1997,** *30*, (24), 7478-7486.

5.0   SUMMARY AND FUTURE WORK

5.1   SUMMARY

Our work in material development of our polymerized crystalline colloidal array (PCCA) sensor materials has led to the development of new photonic crystal hydrogel material compositions, an increased understanding of the sensing mechanism employed in the glucose sensitive PCCA, and a more directed approach to optimization of the swellability of the stimuli-sensitive PCCA materials.

We have developed a new PCCA hydrogel system based on chemically modified poly (vinyl alcohol) (PVA). The PVA polymer chains were modified to incorporate pendant vinyl groups onto the polymer backbone, which can be used to crosslink the polymer via a UV-initiated free radical polymerization. The PVA-based PCCA exhibits efficient diffraction of visible light, most often with increased homogeneity across the hydrogel surface when compared with acrylamide-based PCCA. The PVA-PCCA can be easily functionalized with pendant carboxylic acid groups, which can be further functionalized through simple carbodiimide (EDC) coupling of amine-containing compounds to produce stimuli-responsive photonic crystal materials. Most notably, this material can be dried and then rehydrated by immersion in water, while retaining its diffraction and mechanical properties. This reversibility of rehydration affords practical storage of hydrogel sensors in the dry state, facilitating their future commercialization.

98

We continued the development of our intelligent PCCA (IPCCA) glucose sensing materials for application in monitoring relatively high glucose concentrations. We modified the synthesis and fabrication of our IPCCA to increase the reproducibility of the material. Excluding oxygen from the polymerization process of the PCCA base material has increased our control over the monomer incorporation and increased the homogeneity of absolute diffraction across the surface of the hydrogel. Controlling the pH, through use of a buffered saline solution, and a second addition of EDC during the coupling step has increased the reproducible incorporation of the boronic acid recognition group onto the hydrogel backbone.

The resulting glucose sensor material functions reversibly over a period of one week when stored in a buffered saline solution at room temperature. We demonstrated that the use of a concentrated glucose solution allowed the sensor material to be reversibly dried and rehydrated while retaining its diffraction and sensing properties. In addition, by using independently determined values for the hydrogel effective crosslink density and the association constant of 5-amino-2-fluorophenylboronic acid for glucose, we demonstrated that we could model the diffraction response of our sensing materials, but that the response in the hydrogel matrix is more complicated than that predicted using simple solution equilibria. By varying the concentration of boronic acid incorporated into the material, varying environmental conditions, and challenging the sensing response with interfering species, we significantly increased our understanding of the IPCCA sensing mechanism.

As the swelling properties of hydrogel materials depend on their network structure, which is significantly related to the degree of effective crosslinking within the network, we investigated the mechanical properties of our photonic crystal hydrogels as a function of the polymerization conditions and incorporated CCA particle size. We experimentally determined the shear storage

modulus of the material and used these values to determine the effective crosslink densities. We found that the storage modulus increases linearly with increasing particle size, over the range of sizes studied. As there is no adhesion of the polymer matrix to the embedded particles, we attribute the size dependence of the overall modulus to the increased contribution of slip within the system, owing to the increased surface area of smaller particles. We also found that the storage modulus increases upon exclusion of oxygen during polymerization, and that this increase is more pronounced for hydrogels without CCA inclusions. The effective hydrogel crosslink densities determined from the storage modulus values indicate that we can affect the responsivity of our photonic crystal materials by controlling the included nanoparticle size, providing for a more direct approach to improved PCCA sensor material development.

5.2   FUTURE WORK

5.2.1   Convergence of PVA-PCCA and Glucose-Sensitive IPCCA

In Chapter 2, we demonstrated the utility of a PVA-PCCA as a platform for photonic crystal hydrogel sensor development. The carboxyl-functionality of the polymer backbone facilitates the use of this material in the advanced development of traditionally acrylamide-based sensors, as this is the point of coupling for most molecular recognition groups utilized in those sensors. Owing to the innate biocompatibility of the PVA polymer backbone, this material would best be utilized in the development of IPCCA that are in contact with bodily fluids. In that case, a natural extension of this material would be in the further development of the glucose-sensitive PCCA described in Chapter 3.

Although the use of this material is not straight forward in a boronic acid containing IPCCA, it presents significant advantages that make it worth pursuing. As the PVA backbone contains pendant hydroxyl groups, in essence cis-diols, boronic acid moieties coupled to the hydrogel are capable of complexing to the polymer backbone. This complexation could be utilized for the development of a competitive-binding-based glucose sensing IPCCA. Other groups have demonstrated responsive hydrogels, which utilize a polymer backbone with native hydroxyl groups and incorporated boronic acid moieties, that swell in the presence of glucose[1-6]. Specifically, Lowe et al[2,4] have recently utilized a PVA-based material that swells in the presence of glucose under physiological conditions.

The swelling demonstrated by the various hydrogel systems in the presence of glucose is owed to the initial complexation of tethered boronic acid to the native diols in the hydrogel and the subsequent breaking of this complex, as the boronic acid binds free glucose in solution. By careful tailoring of the concentrations of the competitive binder (native diol) and boronic acid derivatives, it is possible to prepare a material capable of a monotonic and linear swelling response to glucose within the physiological glucose concentration range.

As the concentration of both the native diols and the incorporated boronic acid groups will impact the sensor response, we may have to take an alternative approach to prepare a PVA-based glucose IPCCA, as the native diols in the PVA-based hydrogel are the same hydroxyl groups that are modified for molecular recognition group attachment. It would be more straightforward to utilize an interpenetrating network (IPN) IPCCA: where one network is composed of the PVA-based PCCA containing the native diols and the other network is composed of a polymerizable boronic acid derivative. The use of an IPN would facilitate control of the concentrations of these components individually. In addition, from a practical standpoint,

the use of a second polymerization step for functionalization of the PVA-PCCA is much more feasible for future commercial production than the multiple solvent exchanges and coupling steps used for attachment of the molecular group directly to the PVA polymer backbone.

5.2.2 Extension of PCCA Mechanical Characterization

In Chapter 4, we demonstrated the dependence of our material's effective crosslink density on the size of the embedded nanoparticles. We also noted the apparent domination of effective crosslink density by the nanoparticle inclusions over the covalent crosslinks provided by the bisacrylamide crosslinker. To increase our quantitative understanding of the impact of each of these components on the overall hydrogel swellability, a more thorough investigation is necessary.

We propose a systematic variation of the crosslinker concentration in the prepolymerization solution combined with the variation of sizes of embedded nanoparticles. We will also vary the crosslinker concentration in hydrogels prepared without nanoparticle inclusions. Finally, we will repeat the experimentation with silica nanoparticles, which have been shown to interact with the surrounding hydrogel matrix, even in a PCCA-like material[7]. (We will also repeat the SEM imaging of the PCCA for those containing silica nanoparticles to verify the adhesion of the hydrogel matrix to the embedded particles.) The comparison of the resulting effective crosslink densities should help elucidate the primary mechanism by which the nanoparticle inclusions are affecting the effective crosslink density of the material: the slip of the hydrogel at the nanoparticle surface, the reduction of the overall material strain by incorporation of the rigid particles, or the distribution of the polymer chains during polymerization and resulting polymer chain mobility within the elastomer.

Also, a recent study has indicated that the inclusion of an ordered array of nanoparticles within a hydrogel matrix increases the effective crosslink density to a greater degree than a random dispersion of the same particles[7]. The authors attribute this effect to the increased surface area available on the ordered non-aggregated particles, as they attribute the increase in observed effective crosslink density to the adhesion between the hydrogel matrix and the embedded particles. It would be interesting to determine whether or not there is, in fact, a substructural component to the increase in effective crosslink density observed in our PCCA without hydrogel matrix adhesion to the particles. By preparing PCCA with different sized polystyrene particles, both ordered and disordered (with the use of salt in the prepolymerization solution), we should be able to elucidate whether or not the embedded three-dimensional array imparts an increased stability to the overall material.

5.3   REFERENCES

(1)   Kitano, S.; Koyama, Y.; Kataoka, K.; Okano, T.; Sakurai, Y. *J. Controlled Release* **1992**, *19*, 161-170.

(2)   Domschke, A.; March, W. F.; Kabilan, S.; Lowe, C. *Diabetes Technol. Ther.* **2006**, *8*, 89-93.

(3)   Lee, Y.-J.; Pruzinsky, S. A.; Braun, P. V. *Langmuir* **2004**, *20*, 3096-3106.

(4)   Yang, X.; Lee, M.-C.; Sartain, F.; Pan, X.; Lowe, C. R. *Chem.--Eur. J.* **2006**, *12*, 8491-8497.

(5)   Choi, Y. K.; Jeong, S. Y.; Kim, Y. H. *Int. J. Pharm.* **1992**, *80*, 9-16.

(6)   Hisamitsu, I.; Kataoka, K.; Okano, T.; Sakurai, Y. *Pharm. Res.* **1997**, *14*, 289-293.

(7)   Yanagioka, M.; Frank, C. W. *Macromolecules* **2008**, *41*, 5441-5450.